2.1 Introduction

In recent years, the area of C(sp^2)-H/C(sp^3)-H functionalization, which entails activating inert C(sp^2)-H/C(sp^3)-H bond, has gained significant interest as a novel and atomically efficient technique for straight forward conversion of simple substrate into a helpful molecule. Over the past few decades, the field of catalytic C-H functionalization has expanded rapidly in terms of both the scope of conceivable transformations and the kinds of catalytic manifolds that permit C-H functionalization. Many catalytic techniques have been used for the selective functionalization of C-H bonds, including those using transition metals, enzymatic systems, and photochemical, electrochemical, and photoredox systems [1-9].

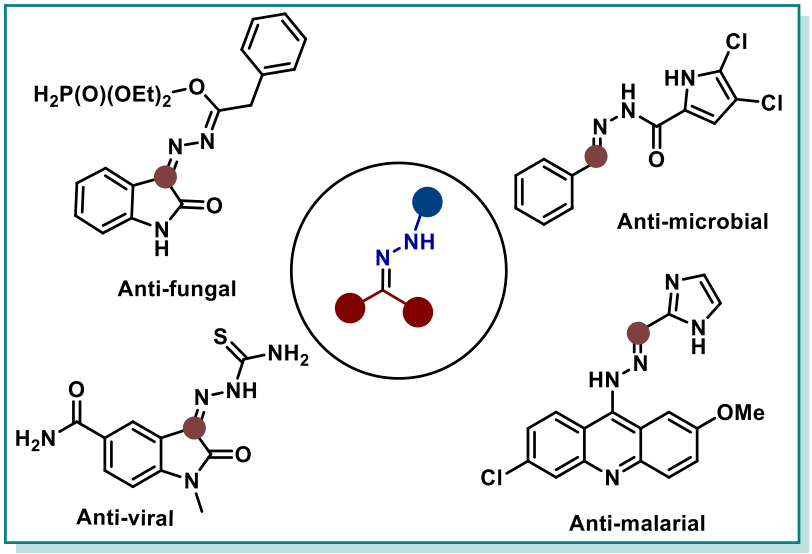

Figure 2.1 Biologically active Hydrazones

Among these, photoredox catalysis is still growing quickly in various areas of scientific studies, including applications to new reaction development, renewable energy, chemical feedstock, natural product synthesis, and biological applications [10-14]. As a green, potent,

and environmentally benign tool for organic synthesis, visible light in conjunction with photoredox catalysis to enable chemical transformations has also become more prominent lately [15-19]. Eosin-Y is a specific organic dye that triggers photoredox catalysis for organic transformations. It has drawn greater attention recently because of its easy handling, environmental friendliness, and significant potential for use in visible-light-mediated organic transformation [20-23].

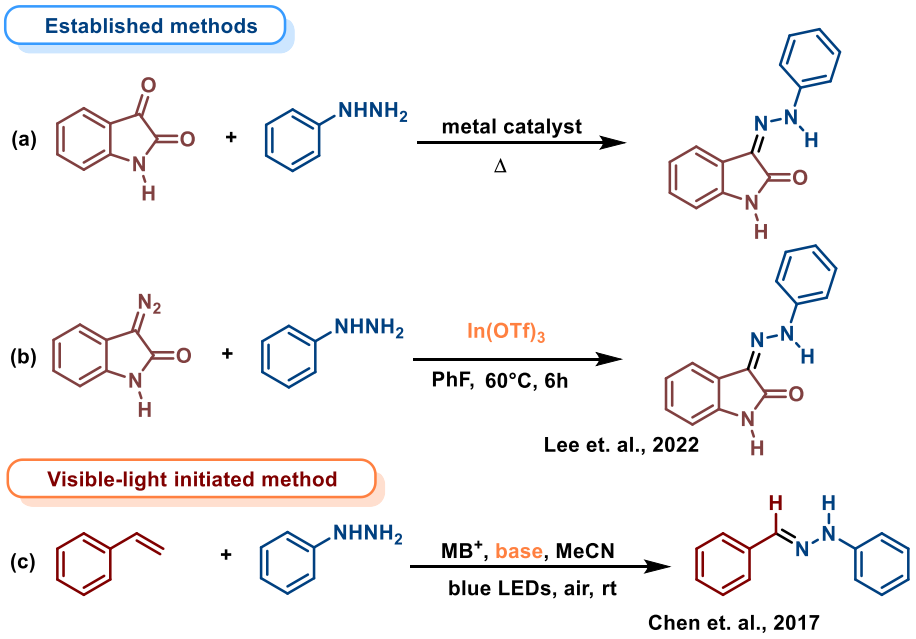

Scheme 2.1 Previous methods for the synthesis of Hydrazones

The creation of C-N bonds, a class of important chemical bonds frequently found in bioactive compounds, natural products, and functional materials, is one of the most successful applications of visible-light photocatalysis [24-27]. Hydrazones are an important class of fundamental organic molecules containing C-N bonds that are valuable building blocks for synthesizing biologically active natural products and functional materials [28-33] (Figure 2.1). These hydrazone derivatives have shown a wide range of biological activities, such as

anti-proliferative [34], monoamine oxidase inhibitory [35], amoebicidal [36], anti-microbial [37], insecticidal [38], anti-inflammatory & analgesic [39], and EGFR inhibitory [40]. These molecules have also been used in chemical synthesis as dyes [41], ligands [42], and fluorescent sensors [43,44]. The addition of hydrazone moieties on the indole ring/aryl group has attracted much attention due to its potential application in photoswitches [45].

Because of their immense relevance, numerous synthetic methods were developed to synthesize these hydrazones [30,31,46,47] (Scheme 2.1). Although these techniques for synthesizing hydrazones were often effective, they have one or more drawbacks, such as thermal conditions, metal catalysts, volatile organic solvents, difficulties in product isolation, and unsatisfactory yields. Therefore, establishing green, gentle, and effective protocols for visible-light-induced C-N coupling using photoredox catalysis is quite exciting and appealing. Hence, we have focused on developing a new methodology for C-N coupling through visible-light-induced sp^2/sp^3 C-H bond functionalization using photocatalysts and atmospheric air as oxidants (Scheme 2.2).

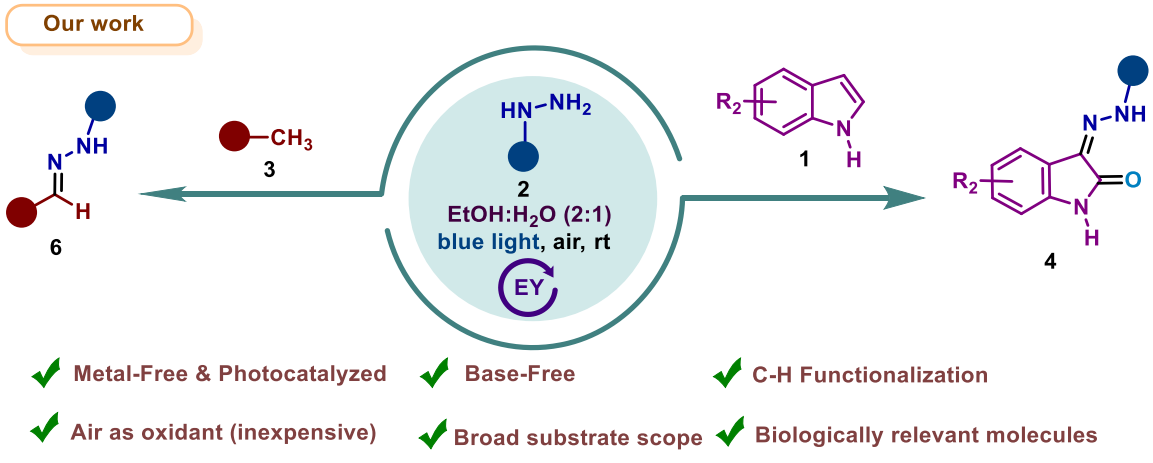

Scheme 2.2 Direct synthesis of hydrazone derivatives

2.2 Results and Discussion

In the initial investigation, the visible-light photoredox C(sp^2)-H functionalization of indole (**1a**) with phenylhydrazine (**2a**) was selected as the model reactant to optimize the reaction conditions under blue LED irradiation in ambient air at room temperature (Table 2.1). Firstly we investigated the role of various photocatalysts (Table 2.1, entries 1-4) using ethanol as a solvent.

Table 2.1 Optimization of reaction parameters [(a)]

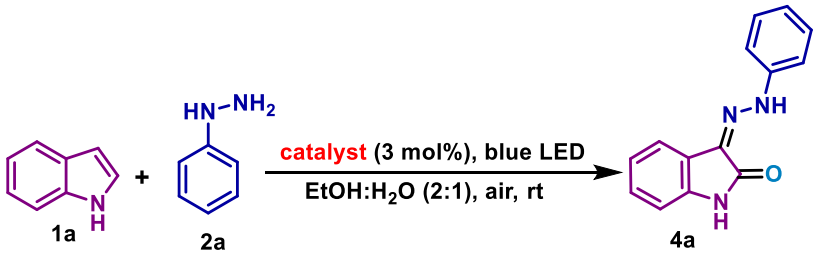

Entry	Catalyst	Solvent	Time (h)	Yield [(b)] (%)
1	Rhodamine B (3)	EtOH	24	4
2	Rose Bengal (3)	EtOH	24	8
3	Xanthone (3)	EtOH	24	5
4	Eosin Y (3)	EtOH	24	42
5	Eosin Y (3)	DMF	24	12
6	Eosin Y (3)	acetonitrile	24	15
7	Eosin Y (3)	methanol	24	22
8	Eosin Y (3)	toluene	24	18
9	Eosin Y (3)	DMSO	24	10

10	Eosin Y (3)	THF	24	20
11	Eosin Y (3)	H_2O	24	45
12	Eosin Y (3)	EtOH: H_2O (1:1)	24	68
13	Eosin Y (3)	EtOH: H_2O (2:1)	24	65
14	Eosin Y (3)	EtOH: H_2O (1:2)	24	88
15	Eosin Y (3)	EtOH: H_2O (1:4)	24	80
16	Eosin Y (1)	EtOH: H_2O (1:2)	24	75
17	Eosin Y (2)	EtOH: H_2O (1:2)	24	81
18	Eosin Y (4)	EtOH: H_2O (1:2)	24	85
19	Eosin Y (3)	EtOH: H_2O (1:2)	26	82
20	Eosin Y (3)	EtOH: H_2O (1:2)	20	78

[(a)]Reaction Condition: indole (0.25 mmol), phenylhydrazine (0.25 mmol), catalyst (3 mol %), solvent (5 mL), blue LED (24 h) under open air at room temperature. [(b)]isolated yield.

We found that eosin Y was the most active catalyst, giving product **3a** in 42% yields (Table 2.1, entry 4). Next, a variety of solvents were optimized (Table 2.1, entries 5-11), and water gave a good yield of 45% (Table 2.1, entry 11). In our favor, the reaction yield was accelerated to 68% using a mixture of ethanol and water in a ratio of 1:1 (Table 2.1, entry 12). Encouraged by the finding, a different ratio of ethanol and water (Table 2.1, entries 12-15) was tried. We got the best result (88%) using a mixture in the ratio of 1:2 (Table 2.1, entry 14).

Further, we varied the loading of eosin Y from 3 mol% to 1, 2, 4 mol% (Table 2.1, entries 16-18) and found a decrease in yield on increasing or decreasing the mol% of the

photocatalyst. We tried extending or shortening the reaction time (Table 2.1, entries 19-20), but we failed to get a better yield of product **4a**.

Table 2.2 Optimization of different colour LED [a]

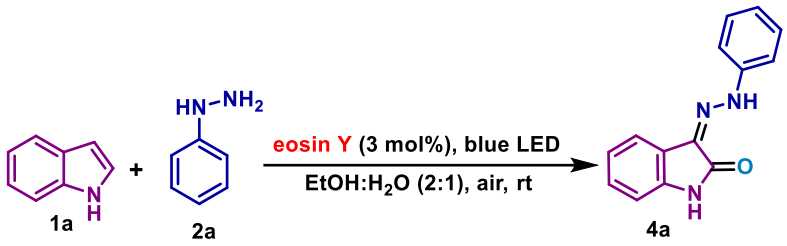

Entry	Variations in the reaction conditions	Yield [b] (%)
1	in dark	nr
2	green LEDs instead of blue LEDs	25
3	purple LEDs instead of blue LEDs	68
4	white LEDs instead of blue LEDs	79
5	20W CFL instead of blue LEDs	74
6	blue LEDs	88
7	under O_2 atmosphere	89

[a]Reaction Condition: indole (0.25 mmol), phenylhydrazine (0.25 mmol), eosin Y (3 mol %), solvent (5 mL), light source (24 h) under open air at room temperature. [b]isolated yield

Furthermore, the effect of light was investigated. Product was not obtained when the reaction was carried out in the dark (Table 2.2, entry 1), demonstrating the significance of light irradiation. Additionally, we used green, purple, and white LED and 20W CFL instead of the blue LED (Table 2.2, entries 2-5) for irradiation and got 25, 68, 79, and 74% yield, respectively. After looking into the impact of the atmospheric air, it was discovered that the

reaction under oxygen practically produced almost the same yield as under air atmosphere (Table 2.2, entry 7).

Table 2.3 Scope of indole for the synthesis of hydrazones [(a)]

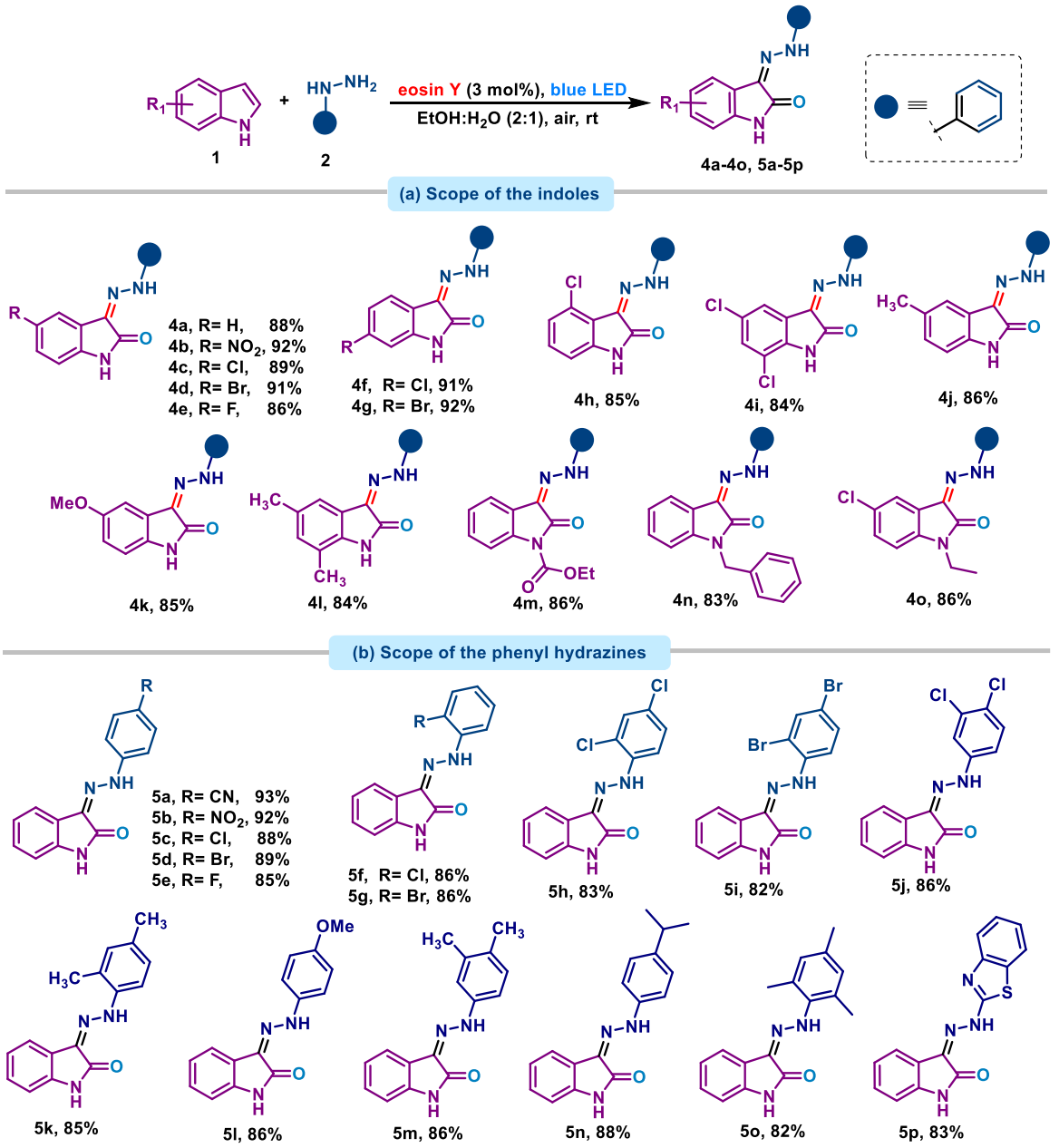

[(a)]Reaction Condition: indoles (0.25 mmol), phenylhydrazine (0.25 mmol), eosin Y (3 mol %), solvent (5 mL), blue LED (24 h) under open air at rt.

This result showed that the atmospheric oxygen molecule or O_2 produced *in-situ* from H_2O_2 (Scheme 2.4) might be crucial to this transition. The optimal conditions were established using 3 mol% of eosin Y in a mixture of ethanol and water in the ratio of 1:2 under blue LED irradiation for 24 hrs in atmospheric air.

After establishing the optimized reaction condition, we shifted our attention toward investigating the substrate scope and generality of different indole, toluene, and phenylhydrazines. As depicted in Table 2.3 (a), the reaction of different indole derivatives with phenylhydrazine was examined (**4a-4o**). Indoles with various electron-withdrawing groups like halides (Cl, Br, F) and nitro give good to excellent yields (84%-92%). Electron-donating groups (methyl and methoxy) were also well tolerated in this transformation, giving 84-86% yields. Additionally, this approach was appropriate with *N*-derivatives of indoles providing targeted products in 83-86% yields (**4m-4o**).

Next, we looked into the range of substrates for the reaction of various arylhydrazine derivatives with indole to deliver the target products in 82-93% yields **(5a-5p)** (Table 2.3 (b)). This transformation effectively tolerated various electron-withdrawing groups (halides, cyano, and nitro) to give excellent yields. Electron-donating groups like methyl, methoxy, isopropyl, and heterocyclic hydrazine provided the desired products in good to excellent yields (82-88%).

Following the effective synthesis of 3-(2-phenylhydrazineylidene)indolin-2-one derivatives, we focused on the synthesis of 1-benzylidene-2-phenylhydrazine derivatives (Table 2.4 (a)) according to the optimized reaction conditions (Table 2.1, entry-14).

Table 2.4 Substrate scope for the synthesis of 1-benzylidene-2-Phenylhydrazines [a]

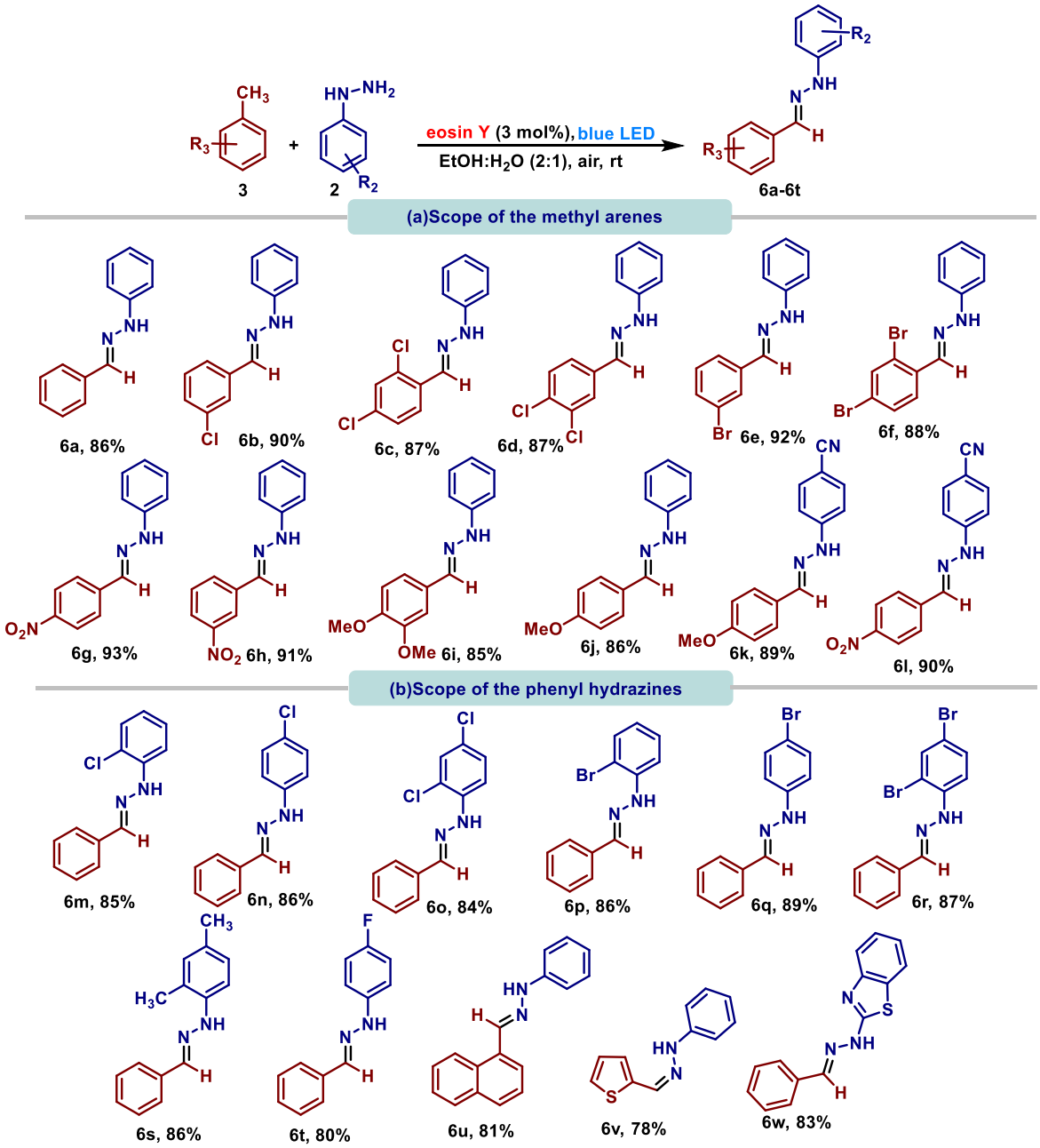

[a]Reaction Condition: toluene (0.25 mmol), phenylhydrazine (0.25 mmol), catalyst (3 mol %), solvent (5 mL), blue LED (24 h) under open air at room temperature.

We tested the range of the substrate using different methylarenes (halides, nitro, and methoxy), 1- methylnaphthalene (**6u**), and methyl-heteroarene (**6v**), and we observed that all

of these derivatives performed well and produced the desired product in yields of 85–93%. The reactivity of arylhydrazines with methylarenes was then assessed (**6k-6t**). It was found that, similarly, in table 2.4 (b), various arylhydrazines were well tolerated by functional groups such as methyl, cyano, as well as halides (Cl, Br, and F) and heterocyclic hydrazine (**6w**), providing a wealth of opportunity for further functionalization.

2.3 Control Experiment

After evaluating the reproducibility and sensitivity of the substrate scope, we moved our attention toward the mechanism of the reaction and conducted several mechanistic investigations (Scheme 2.3). Furthermore, the UV-visible spectra of reactants (**1a**, **2a**, and **3a**), reaction mixtures (**1a**+**2a**, **2a**+**3a**), and eosin Y were observed (Figure 2.2a, b). The finding showed that, except for the reactants, the photocatalyst eosin Y and the reaction mixture could absorb blue light.

Next, the results of subsequent Stern-Volmer experiments showed that excited eosin Y was successfully quenched by **2a** (Figure 2.3). As seen in Figure 2.3, the quenching effect gets more pronounced as the concentration of **2a** rises. It was discovered that there was a linear relationship between the concentration of **2a** and Io/I (Io and I are the fluorescence intensity) prior to and following the addition of **2a** (Figure 2.4). The outcomes showed that **2a** was an effective quencher for excited eosin Y.

As depicted in Scheme 2.3, under N_2 atmosphere (Scheme 2.3, entry a) the reaction was unable to produce the desired products **4a** and **6a**, proving that O_2 was crucial to the reaction's success.

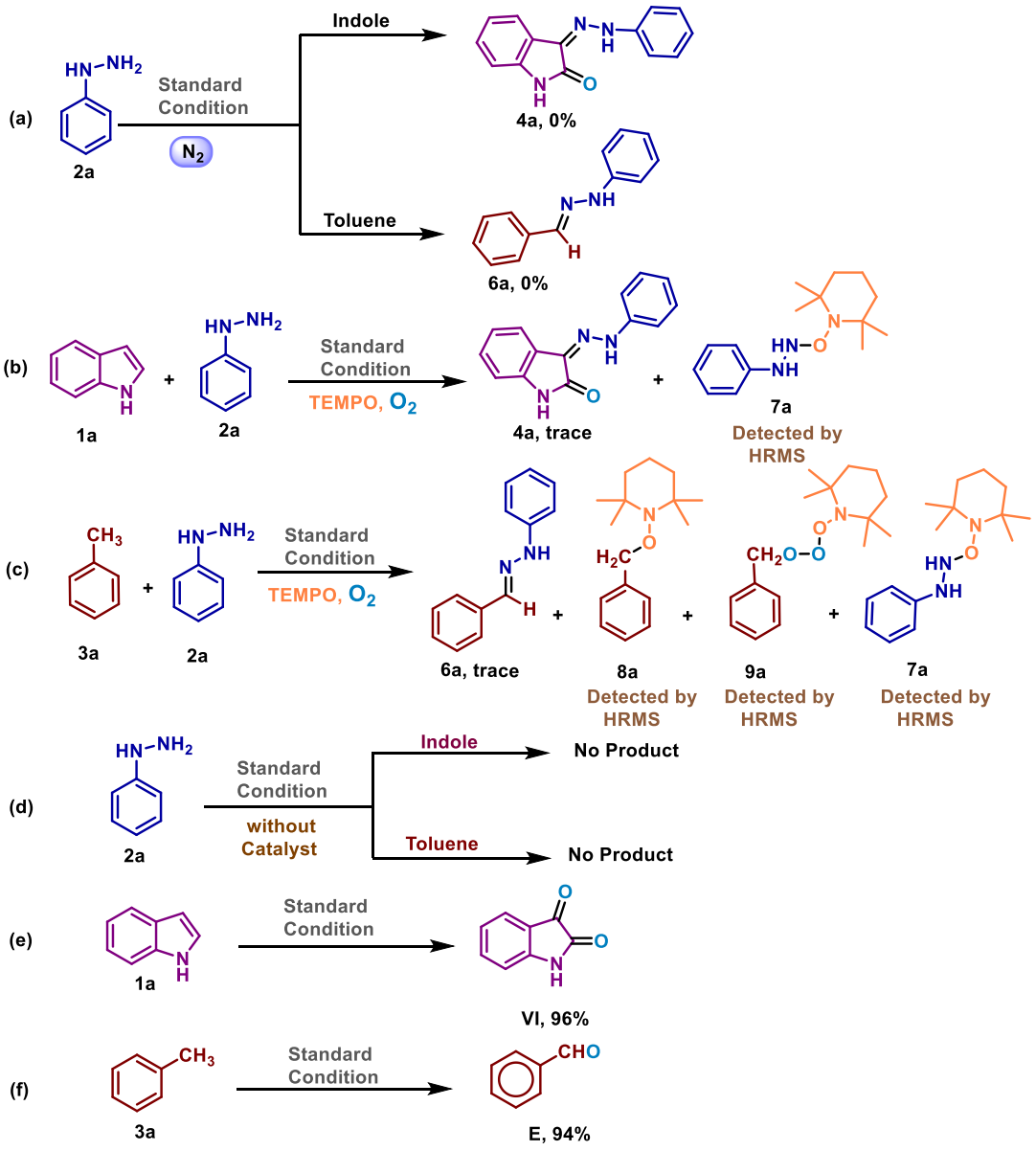

Scheme 2.3 Mechanistic Investigation

Then, a radical scavenger 2, 2, 6, 6-tetramethylpiperidin-1-oxyalkyl (TEMPO) was introduced to the process (Scheme 2.3, entries b, c), and we found that the yields of products **4a** and **6a** were greatly suppressed. HRMS data confirmed the formation of adducts **7a**, **8a**, and **9a**. It suggests that the PhNHNH free radical was formed, and the reaction follows the

free radical mechanism. To get the insight of intermediate, the analysis of the reaction under standard conditions was done, and we got intermediate **VI** (isatin) and **E** (benzaldehyde) (Scheme 2.3, entries e and f). The formation of intermediate **VI** and **E** was confirmed by ^{1}H and ^{13}C NMR spectroscopy.

Reaction in the absence of a catalyst gives no product indicating that photocatalyst plays a vital role (Scheme 2.3, entry d). Additionally, light-dark cycle experiments showed that this reaction required exposure to light irradiation (Figure 2.6). The quantum yield was found to be 0.0074 (Figure 2.5). These experimental findings showed that the reaction was light-dependent and ruled out the idea of radical chain propagation ($\phi \leq 1$).

2.3.1 UV-Vis absorption experiment

The sample was prepared by mixing of **1a**, **2a** and mixture (**1a**+**2a**) (Figure 2.2a) and **3a**, **2a** and mixture (**2a**+**3a**) (Figure 2.2b) in methanol solvent [Conc. reaction mixture = 1.25×10^{-4}mol/L] in a light path quartz UV cuvette.

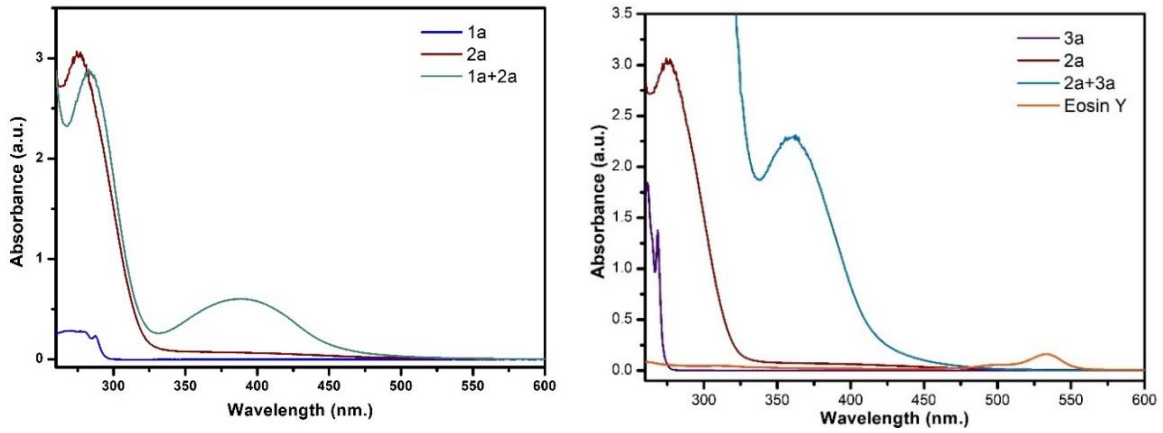

Figure 2.2 a) UV-vis absorption spectra of (**1a**+**2a**), **b)** UV-vis absorption spectra of (**2a**+**3a**)

2.3.2 Stern-Volmer Fluorescence Quenching Studies

In a Fluorescence experiment, the solution of EY in ethanol was added to the appropriate amount of **2a**. The addition of **2a** was repeated 6 consecutive times. We recorded the emission spectra after each addition. All the solutions were excited at **559 nm,** and the emission was acquired from 0 nm to 700 nm. The result shown in Figure 2.3 indicates that **2a** quenches the excited state of EY and its emission.

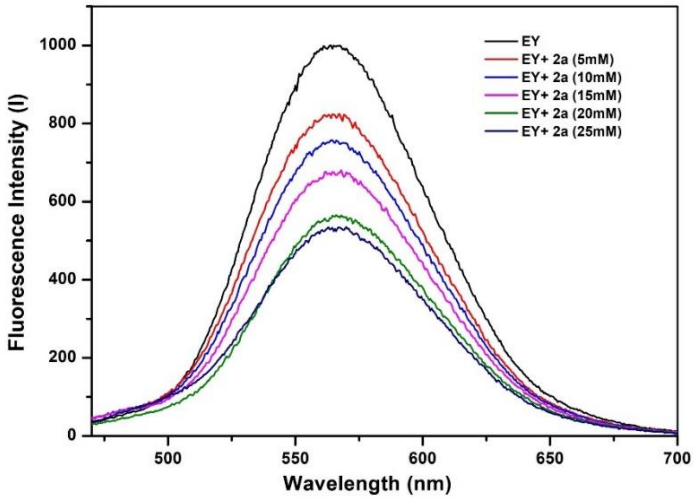

Figure 2.3 The fluorescence emission spectra of EY with different conc. of quencher **2a**

The Stern-Volmer plot (Figure 2.4) indicated a linear relationship between the concentration of 2a and the ratio I_0/I. The Stern-Volmer constant K_{SV} was calculated using equation 1.

$I_0/I = 1 + K_{SV}[Q]$ …….**Eq. 1**

Where, I_0 = the intensity of fluorescence of EY, without quencher 2a

I = the intensity of fluorescence of EY, with quencher 2a

[Q] = concentration of the quencher 2a

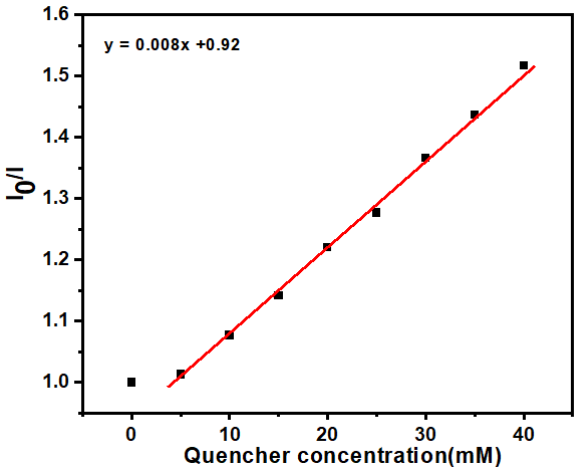

Figure 2.4 Stern-Volmer fluorescence quenching plot

2.3.3 Quantum Yields

The quantum yield was recorded on a PerkinElmer LS 55 Fluorescence spectrometer. 1.0 mM stock solution of **4a** was prepared and diluted with ethanol. The solution was placed in a screw top 1cm quartz cuvette, and emission spectra of the sample were collected. The excitation wavelength was fixed at 395nm (Figure 2.5).

Estimation of Quantum Yields: The quantum yield of probe ***DPA*** and ***DPA***+N_2H_4 with respect to quinine sulfate (Φ = 0.54, 1M H_2SO_4) as an internal standard was estimated by using the equation

$$\mathbf{Q = Q_R.\ \mathit{I}/\mathit{I}_R.\ OD_R/OD.\ n^2/n^2_R}$$

Where Q is the quantum yield, *I* stand for the integrated area of fluorescence intensities, OD is optical densities, and *n* is the refractive indexes of solution. The subscript *R* refers to the reference fluorophore of known quantum yield.

Quantum Yields Φ =0.0074

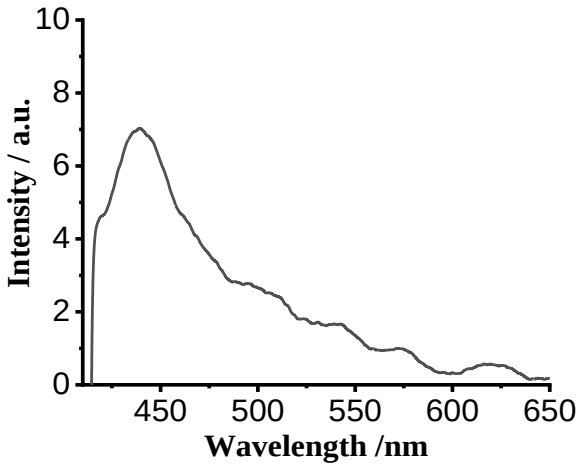

Figure 2.5 Quantum yield

2.3.4 ON-OFF Experiments

The reaction between **1a** and **2a** was conducted under the standard conditions on a 0.25 mmol scale. The reaction mixture was subjected to sequential periods of stirring under visible-light-irradiation (blue LED) followed by stirring in the absence of light. At each time point, one reaction system was suspended, which was then purified with column chromatography to give the corresponding products **3a**. The yield of **3a** was measured by weight of the product (Figure 2.6).

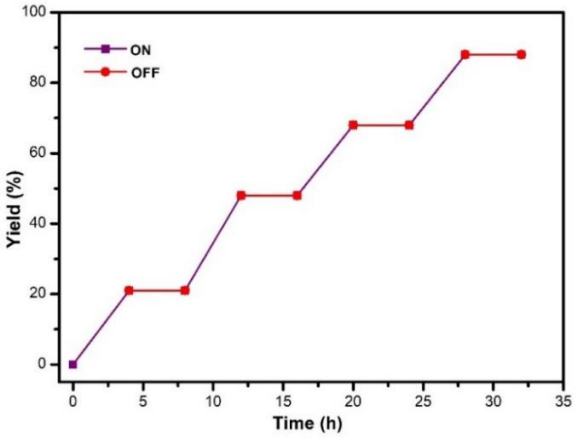

Fig 2.6 ON-OFF Experiments

2.4 Proposed Mechanism

A potential reaction mechanism for photocatalyzed C(sp^2)-H (Scheme 2.4) functionalization (oxidative coupling) was hypothesized based on the outcomes of the control experiments and previous literature [48-50].

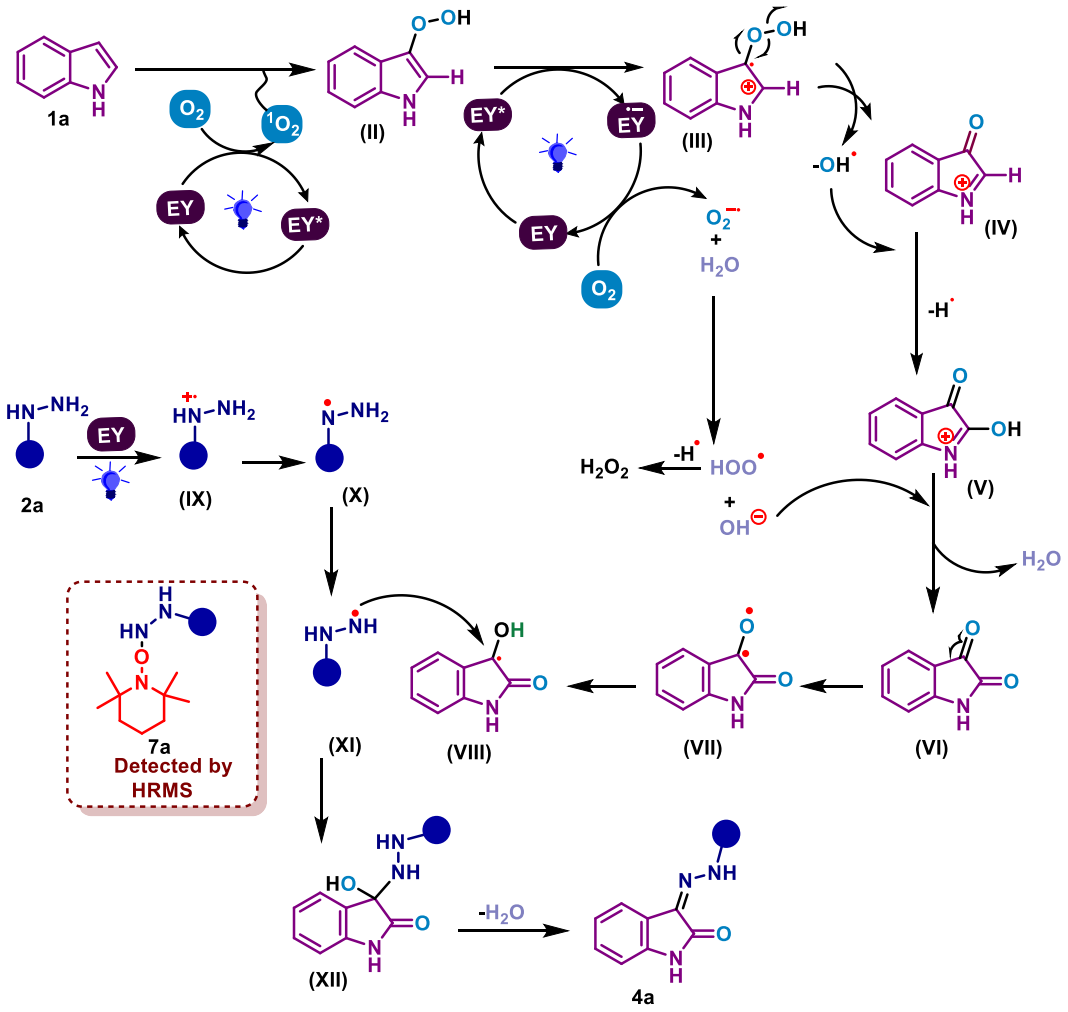

Scheme 2.4 Plausible mechanism for C(sp^2)-H functionalization

Excited eosin Y (EY*) is created from eosin Y (EY) when it is exposed to visible light. Singlet oxygen is formed from oxygen as oxygen quenches excited eosin Y (EY*). This singlet oxygen interacts with indole (**1a**) to form peroxo species **II**. In the second

photocatalytic cycle, the oxidized species **II** produces the radical anion $EY^{\bullet-}$ and the peroxoindole species **III**. The cleavage of species **III** results in the successive formation of cation **IV** and hydroxyl radical. The hydroxyl radical that is created in this way removes an atom of hydrogen from **IV**. The superoxide radical anion is formed when $EY^{\bullet-}$ is reduced by oxygen. When this radical anion reacts with water, it produces hydroxide anions and peroxide radicals. Species **V** is formed from the reaction of hydroxyl radical and the oxidized form of species **IV**. Intermediate **VI** is formed from species **V** by the loss of water molecules. Also, phenylhydrazine (**2a**) gets converted to ionic radical (**IX**). This ionic radical gets converted into radical (**X**) upon deprotonation. Upon rearrangement, radical (**XI**) is formed from (**X**). Radical (**XI**) reacts with intermediate **VI** to form desired product **4a** by removal of water.

The plausible mechanism for photoredox C(sp^3)-H (Scheme 2.5) functionalization was also proposed. When exposed to blue light, the photocatalyst eosin Y (EY) enters its excited state, which results in the formation of the potent photooxidant EY*. This species goes through a single electron transfer (SET) step with methylarene (**3a**), producing the radical cationic intermediate **A**. The reduced EY reaches its ground state by transferring its electron to O_2, which in turn converts to superoxide ion. This superoxide ion combines with H_2O and produces hydrogen peroxide and O_2 molecules (this O_2 helps in increasing the yield of the reaction). The cationic intermediate **A** undergoes proton abstraction generating benzylic radical **B**. This is then trapped by oxygen, resulting in peroxo-species **C**, which, following H-radical abstraction, results in benzyl hydroperoxide **D**. This species leads to the formation of intermediate **E** after the removal of a water molecule. Phenylhydrazine reacts with

intermediate **E** to give the desired product **6a** in a similar manner. This mechanism is supported by the formation of complex **8a** and **9a** (Scheme 2.3).

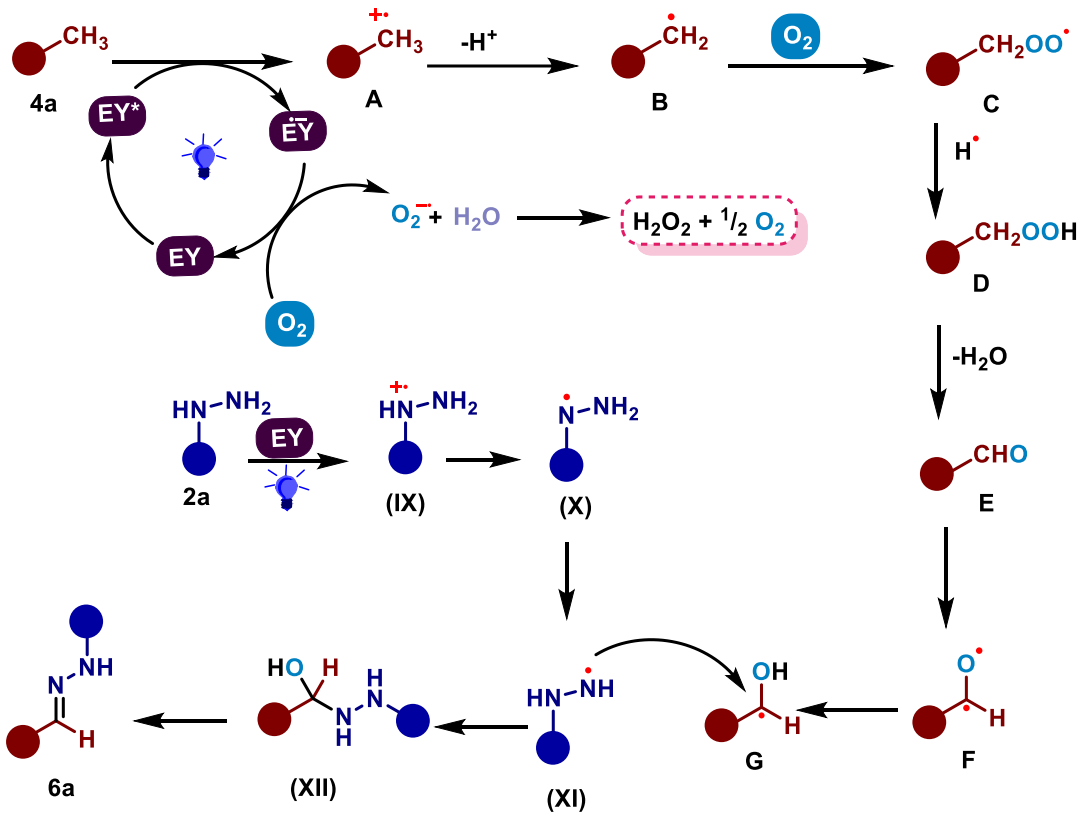

Scheme 2.5 Plausible mechanism for C(sp^3)-H functionalization

2.5 Conclusions

In summary, we have developed a highly efficient, green, and metal-free method for synthesizing arylhydrazones through oxidative C-H functionalization to form C-N bonds under ambient air using organic photoredox catalysis at room temperature. The current technique has several benefits, including low cost, high efficiency, and tolerance of a wide range of functional groups for indoles, methylarenes, and arylhydrazines, and several arylhydrazones were synthesised in good to moderate yields. The detailed mechanistic

investigation demonstrated that the reaction proceeds through photoredox catalysis, and the formation of intermediates reflects the C-H functionalization. Such easy and controlled photocatalytic techniques may open the door to the related transformation of arylhydrazines.

2.6 Experimental Procedures

2.6.1 General procedure for the preparation of compounds 4a-4o and 5a-5p.

A 25 mL RB flask equipped with a magnetic stirring bar was charged with indole derivatives **1** (0.25 mmol), eosin Y (3 mol%), and solvent (5 mL). The mixture was then stirred at room temperature and irradiated with blue LEDs light strips for 6 h under open air. After that, phenylhydrazine derivatives **2** (0.25 mmol) were added to the reaction mixture. The progress of the reaction was monitored via TLC. The precipitate obtained was filtered and washed with ethanol after the completion of the reaction. The desired product was obtained in good yields after recrystallization using ethanol.

2.6.2 General procedure for the preparation of compounds 6a-6w.

A 25 mL RB flask equipped with a magnetic stirring bar was charged with methylarenes **3** (0.25 mmol), eosin Y (3 mol%), and solvent (5 mL). The mixture was then stirred at room temperature and irradiated with blue LEDs light strips for 6 h under open air. After that phenyl hydrazine derivatives **2** (0.25 mmol) were added to the reaction mixture. The progress of the reaction was monitored via TLC. The precipitate obtained was filtered and washed with ethanol after the completion of the reaction. The desired product was obtained in good yields after recrystallization using ethanol.

2.7 Characterization of products

3-(2-Phenylhydrazineylidene)indolin-2-one (4a)

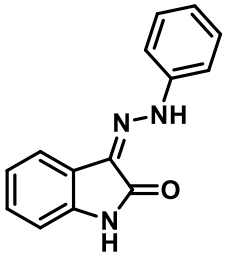

88% yield; dark yellow solid; m.p. 218-219°C; **^{1}H NMR** (500 MHz, DMSO-d_6) δ 12.75 (s, 1H), 11.03 (s, 1H), 7.56 (d, *J* = 7.3 Hz, 1H), 7.43 (d, *J* = 7.6 Hz, 2H), 7.39 (d, *J* = 7.3 Hz, 2H), 7.25 (t, *J* = 7.7 Hz, 1H), 7.08 – 7.04 (m, 2H), 6.93 (d, *J* = 7.8 Hz, 1H). **^{13}C NMR** (126 MHz, DMSO-d_6) δ 163.65, 142.98, 140.28, 129.97, 128.99, 128.16, 123.39, 122.36, 121.63, 119.10, 114.55, 110.99. **HRMS** (ESI) m/z: $[M+H]^+$ calculated for $C_{14}H_{11}N_3O$: 238.0902; found: 238.0900.

5-Nitro-3-(2-phenylhydrazineylidene)indolin-2-one (4b)

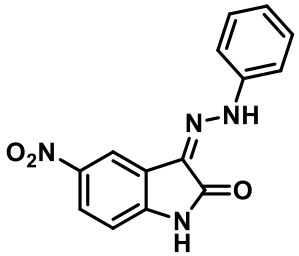

92% yield; yellowish brown; m.p. 280-281°C; **^{1}H NMR** (500 MHz, DMSO-d_6) δ 12.75 (s, 1H), 11.67 (s, 1H), 8.33 (d, *J* = 2.3 Hz, 1H), 8.18 (m, *J* = 8.6 Hz, 1H), 7.57 (m, *J* = 8.6 Hz, 2H), 7.41 (m, *J* = 7.8 Hz, 2H), 7.12 (m, *J* = 8.2 Hz, 2H). **^{13}C NMR** (126 MHz, DMSO-d_6) δ 163.77, 145.13, 142.90, 142.57, 129.98, 126.06, 124.77, 124.39, 122.45, 115.39, 114.02, 111.05. **HRMS** (ESI) m/z: $[M+H]^+$ calculated for $C_{14}H_{10}N_4O_3$:283.0753; found: 283.0757.

5-Chloro-3-(2-phenylhydrazineylidene)indolin-2-one (4c)

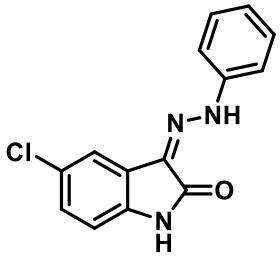

89% yield; yellow solid; m.p. 270-271°C; **^{1}H NMR** (500 MHz, DMSO-d_6) δ 12.75 (s, 1H), 11.15 (s, 1H), 7.58 (d, *J* = 7.1 Hz, 1H), 7.49 (d, *J* = 7.8 Hz, 2H), 7.39 (m, *J* = 7.8 Hz, 2H), 7.28 (m, *J* = 8.3 Hz, 1H), 7.09 (d, *J* = 7.3 Hz, 1H), 6.94 (d, *J* = 8.3 Hz, 1H). **^{13}C NMR**

(126 MHz, DMSO-d_6) δ 163.42, 142.76, 138.80, 129.95, 128.23, 126.95, 126.58, 123.88, 123.46, 118.66, 114.96, 112.40. **HRMS** (ESI) m/z: $[M+H]^+$ calculated for $C_{14}H_{11}N_3O$: 238.0902; found: 238.0900.

5-Bromo-3-(2-phenylhydrazineylidene)indolin-2-one (4d)

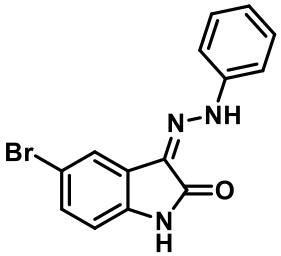

91% yield; brown solid; m.p. 265-267°C. **^{1}H NMR** (500 MHz, DMSO-d_6) δ 12.75 (s, 1H), 11.15 (s, 1H), 7.58 (d, *J* = 2.0 Hz, 1H), 7.49 (d, *J* = 7.7 Hz, 2H), 7.39 (t, *J* = 7.9 Hz, 2H), 7.27 (m, *J* = 8.3 Hz, 1H), 7.08 (s, 1H), 6.93 (d, *J* = 8.3 Hz, 1H). **^{13}C NMR** (126 MHz, DMSO-d_6) δ 163.42, 142.76, 138.81, 129.94, 128.23, 126.96, 126.58, 123.87, 123.46, 118.66, 114.96, 112.39. **HRMS** (ESI) m/z: $[M+H]^+$ calculated for $C_{14}H_{10}N_3BrO$: 316.0007; found: 316.0006.

5-Fluoro-3-(2-phenylhydrazineylidene)indolin-2-one (4e)

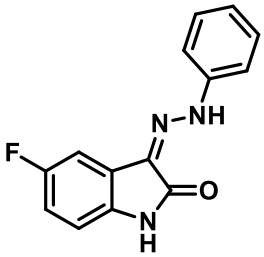

86% yield; reddish solid; m.p. 251-253°C; **^{1}H NMR** (500 MHz, DMSO-d_6) δ 12.77 (s, 1H), 11.12 (s, 1H), 7.81 (d, *J* = 8.8 Hz, 2H), 7.64 (d, *J* = 8.9 Hz, 3H), 7.46 – 7.42 (m, 1H), 7.15 – 7.09 (m, 1H), 6.92 (dd, *J* = 8.5, 4.2 Hz, 1H). **^{13}C NMR** (126 MHz, DMSO-d_6) δ 163.43, 159.69, 146.69, 137.41, 134.25, 130.59, 122.55, 119.75, 116.41, 116.22, 115.28, 112.10, 107.10, 106.90, 104.69. **^{19}F NMR** (471 MHz, DMSO-d_6) δ -121.15, -121.16. **HRMS** (ESI) m/z: $[M+H]^+$ calculated for $C_{14}H_{10}FN_3O$ 256.0808; found: 256.0809.

6-Chloro-3-(2-phenylhydrazineylidene)indolin-2-one (4f)

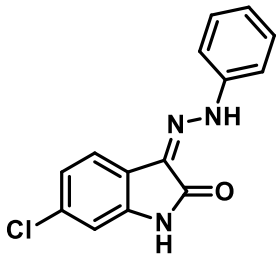

91% yield; yellowish solid; m.p. 264-265°C; **^{1}H NMR** (500 MHz, DMSO-d_6) δ 12.80 (s, 1H), 11.09 (s, 1H), 7.54 (d, *J* = 7.5 Hz, 1H), 7.52 – 7.40 (m, 3H), 7.24 (m, *J* = 8.3 Hz, 1H), 6.99 – 6.97 (m, 2H), 6.92 (d, *J* = 8.3 Hz, 1H). **^{13}C NMR** (126 MHz, DMSO-d_6) δ 163.44, 156.39, 138.29, 136.38, 127.60, 126.43, 125.57, 123.67, 118.22, 116.37, 115.24, 112.24. **HRMS** (ESI) m/z: $[M+H]^+$ calculated for $C_{14}H_{10}ClN_3O$: 272.0512; found: 272.0514.

6-Bromo-3-(2-phenylhydrazineylidene)indolin-2-one (4g)

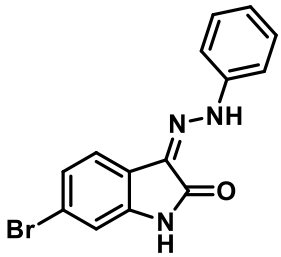

92% yield; yellowish solid; m.p. 270-272°C; **^{1}H NMR** (500 MHz, DMSO-d_6) δ 12.79 (s, 1H), 11.09 (s, 1H), 7.67 (d, *J* = 7.9 Hz, 1H), 7.52 – 7.41 (m, 3H), 7.37 (m, *J* = 8.3 Hz, 1H), 6.99 – 6.96 (m, 2H), 6.88 (d, *J* = 8.3 Hz, 1H). **^{13}C NMR** (126 MHz, DMSO-d_6) δ 163.27, 156.40, 138.65, 136.39, 130.38, 125.40, 124.11, 120.98, 116.40, 115.13, 114.13, 112.74. **HRMS** (ESI) m/z: $[M+H]^+$ calculated for $C_{14}H_{10}BrN_3O$: 316.0007; found: 316.0009.

Chloro-3-(2-phenylhydrazineylidene)indolin-2-one (4h)

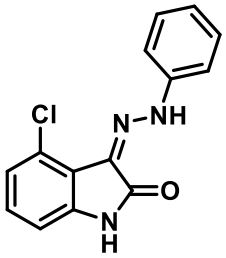

85% yield; yellowish solid; m.p. 263-264°C; **^{1}H NMR** (500 MHz, DMSO-d_6) δ 13.11 (s, 1H), 11.17 (s, 1H), 7.82 (m, *J* = 8.2 Hz, 1H), 7.61 (m, *J* = 7.5 Hz, 1H), 7.51 (m, *J* = 8.0 Hz, 1H), 7.45 – 7.40 (m, 1H), 7.31 (m, *J* = 7.7 Hz, 1H), 7.11 – 7.04 (m, 2H), 6.96 (d, *J* = 7.8 Hz, 1H). **^{13}C NMR** (126 MHz, DMSO-d_6) δ 163.83, 140.96, 139.25, 130.09, 129.87, 129.06, 123.76, 122.57, 119.71, 118.64, 114.60, 111.26. **HRMS** (ESI) m/z: $[M+H]^+$ calculated for $C_{14}H_{10}ClN_3O$: 272.0512; found: 272.0514.

5,7-Dichloro-3-(2-phenylhydrazineylidene)indolin-2-one (4i)

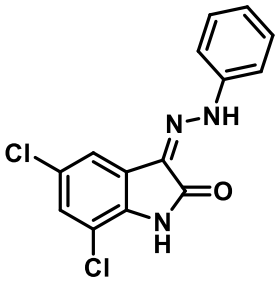

84% yield; dark brown solid; m.p. 258-259°C; **^{1}H NMR** (500 MHz, DMSO-d_6) δ 13.09 (s, 1H), 11.20 (s, 1H), 7.80 (d, *J* = 8.9 Hz, 1H), 7.69 (d, *J* = 8.3 Hz, 1H), 7.61 (d, *J* = 7.2 Hz, 1H), 7.49 (m, *J* = 8.8 Hz, 1H), 7.32 (m, *J* = 7.7 Hz, 1H), 7.09 (m, *J* = 7.6 Hz, 1H), 6.96 (d, *J* = 7.8 Hz, 1H). **^{13}C NMR** (126 MHz, DMSO-d_6) δ 163.84, 141.17, 138.52, 131.61, 130.16, 129.43, 126.50, 122.66, 120.85, 119.90, 115.68, 111.34. **HRMS** (ESI) m/z: $[M+H]^+$ calculated for $C_{14}H_9Cl_2N_3O$: 306.0123; found: 306.0124.

5-Methyl-3-(2-phenylhydrazineylidene)indolin-2-one (4j)

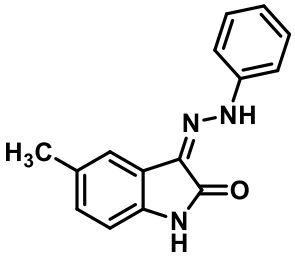

86% yield; yellow solid; m.p. 251-252°C; **^{1}H NMR** (500 MHz, DMSO-d_6) δ 12.73 (s, 1H), 10.92 (s, 1H), 7.43 (d, *J* = 7.5 Hz, 2H), 7.40 – 7.36 (m, 3H), 7.05 (m, *J* = 8.3 Hz, 2H), 6.82 (d, *J* = 7.9 Hz, 1H), 2.32 (s, 3H). **^{13}C NMR** (126 MHz, DMSO-d_6) δ 163.77, 143.04, 138.11, 131.28, 129.95, 129.49, 128.31, 123.28, 121.67, 119.54, 114.49, 110.74, 21.19. **HRMS** (ESI) m/z: $[M+H]^+$ calculated for $C_{15}H_{13}N_3O$: 252.1059; found: 252.1057.

5-Methoxy-3-(2-phenylhydrazineylidene)indolin-2-one (4k)

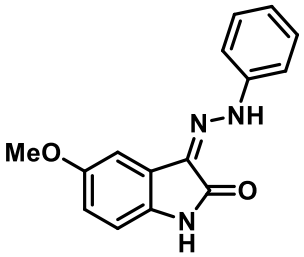

85% yield; dark brown solid; m.p. 245-247°C; **^{1}H NMR** (500 MHz, DMSO-d_6) δ 12.79 (s, 1H), 10.85 (s, 1H), 7.45 (d, *J* = 7.7 Hz, 2H), 7.38 (t, *J* = 7.9 Hz, 2H), 7.15 (s, 1H), 7.05 (s, 1H), 6.84 (d, *J* = 7.1 Hz, 2H), 3.78 (s, 3H). **^{13}C NMR** (126 MHz, DMSO-d_6) δ 163.87, 155.56, 142.95, 134.06, 129.94, 128.49, 123.39, 122.44, 115.27, 114.60, 111.69,

104.34, 56.01. **HRMS** (ESI) m/z: $[M+H]^+$ calculated for $C_{15}H_{13}N_3O_2$:268.1008; found: 268.1009.

5,7-Dimethyl-3-(2-phenylhydrazineylidene)indolin-2-one (4l)

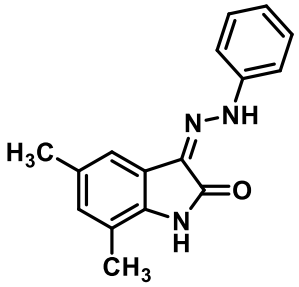

84% yield; white solid; m.p. 256-258°C; **^{1}H NMR** (500 MHz, DMSO-d_6) δ 12.95 (s, 1H), 11.07 (s, 1H), 7.61 – 7.55 (m, 2H), 7.25 (m, *J* = 7.7 Hz, 1H), 7.12 – 7.04 (m, 3H), 6.95 (d, *J* = 7.8 Hz, 1H), 2.26 (d, *J* = 5.2 Hz, 6H). **^{13}C NMR** (126 MHz, DMSO-d_6) δ 164.05, 140.01, 138.51, 132.10, 131.78, 128.75, 128.28, 122.89, 122.34, 118.95, 112.89, 111.05, 20.83, 16.77. **HRMS** (ESI) m/z: $[M+H]^+$ calculated for $C_{16}H_{15}N_3O$: 266.1215; found: 266.1217.

Ethyl-2-oxo-3-(2-phenylhydrazineylidene)indoline-1-carboxylate (4m)

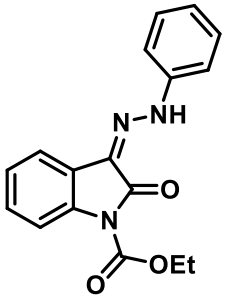

86% yield; pale yellow solid; m.p. 284-285°C. **^{1}H NMR** (500 MHz, DMSO-d_6) δ 12.58 (s, 1H), 7.66 – 7.63 (m, 1H), 7.49 (d, *J* = 7.7 Hz, 2H), 7.39 (d, *J* = 8.4 Hz, 2H), 7.33 (t, *J* = 7.7 Hz, 1H), 7.16 (m, *J* = 7.5 Hz, 2H), 7.08 (t, *J* = 7.3 Hz, 1H), 4.20 (s, 3H), 1.23 (d, *J* = 7.1 Hz, 3H). **^{13}C NMR** (126 MHz, DMSO-d_6) δ 168.54, 154.11, 145.74, 142.85, 134.26, 131.50, 129.97, 126.64, 123.14, 114.88, 110.01, 61.74, 14.52. **HRMS** (ESI) m/z: $[M+H]^+$ calculated for $C_{17}H_{15}N_3O_3$: 310.1113; found: 310.1114.

1-Benzyl-3-(2-phenylhydrazineylidene)indolin-2-one (4n)

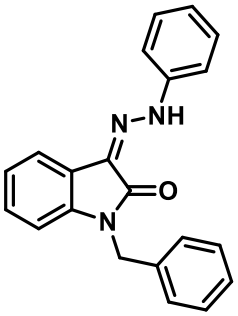

83% yield; light brown solid; m.p. 277-278°C; **^{1}H NMR** (500 MHz, DMSO-d_6) δ 12.73 (s, 1H), 7.63 (d, *J* = 7.4 Hz, 1H), 7.49 (d, *J* = 7.7 Hz, 2H), 7.42 – 7.33 (m, 6H), 7.30 – 7.25 (m, 2H), 7.12 – 7.07 (m, 2H), 5.04 (s, 2H). **^{13}C NMR** (126 MHz, DMSO-d_6) δ 161.63, 142.91, 140.55, 136.84, 129.98, 129.19, 128.84, 128.00, 127.86, 123.66, 123.00, 121.05, 118.99, 114.80, 110.28, 42.80. **HRMS** (ESI) m/z: $[M+H]^+$ calculated for $C_{21}H_{17}N_3O$: 328.1372; found: 328.1374.

5-Chloro-1-ethyl-3-(2-phenylhydrazineylidene)indolin-2-one (4o)

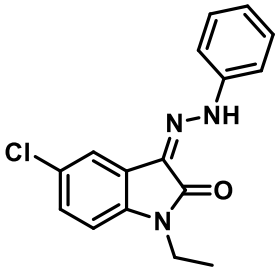

86% yield; yellow solid; m.p. 280-281°C; **^{1}H NMR** (500 MHz, DMSO-d_6) δ 12.70 (s, 1H), 7.85 – 7.76 (m, 3H), 7.69 – 7.66 (m, 3H), 7.40 (m, J = 8.4 Hz, 1H), 7.22 (d, J = 8.4 Hz, 1H), 3.82 (d, J = 7.2 Hz, 2H), 1.21 (s, 3H). **^{13}C NMR** (126 MHz, DMSO-d_6) δ 160.74, 146.62, 139.97, 134.22, 129.24, 129.01, 127.29, 122.37, 119.72, 119.44, 115.47, 111.49, 104.90, 31.77, 13.23. **HRMS** (ESI) m/z: $[M+H]^+$ calculated for $C_{16}H_{14}ClN_3O$: 299.0825; found: 299.0823.

4-(2-(2-Oxoindolin-3-ylidene)hydrazineyl)benzonitrile (5a)

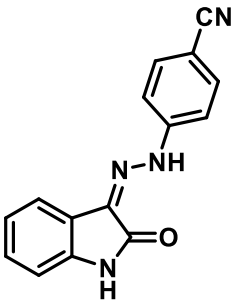

93% yield; white solid; m.p. 241-243°C; **^{1}H NMR** (500 MHz, DMSO-d_6) δ 12.76 (s, 1H), 11.12 (s, 1H), 7.82 – 7.78 (m, 2H), 7.61 – 7.57 (m, 3H), 7.32 – 7.28 (m, 1H), 7.08 (m, *J* = 7.6 Hz, 1H), 6.93 (d, *J* = 7.8 Hz, 1H). **^{13}C NMR** (126 MHz, DMSO-d_6) δ 163.33, 146.86, 141.26, 134.27,

131.15, 130.16, 122.59, 121.15, 119.91, 119.82, 114.95, 111.19, 104.24. **HRMS** (ESI) m/z: $[M+H]^+$ calculated for $C_{15}H_{10}N_4O$ 263.0855; found: 263.0854.

3-(2-(4-Nitrophenyl)hydrazineylidene)indolin-2-one (5b)

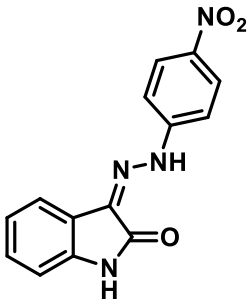

92% yield; reddish solid; m.p. 247-249°C; **^{1}H NMR** (500 MHz, DMSO-d_6) δ 12.72 (s, 1H), 11.01 (s, 1H), 7.55 (d, *J* = 7.1 Hz, 1H), 7.49 (m, *J* = 9.1 Hz, 2H), 7.27 – 7.20 (m, 3H), 7.06 (m, *J* = 7.5 Hz, 1H), 6.93 (d, *J* = 7.7 Hz, 1H). **^{13}C NMR** (126 MHz, DMSO-d_6) δ 163.53, 140.30, 128.97, 128.12, 122.32, 121.65, 119.08, 116.66, 116.48, 116.16, 116.09, 110.96. **HRMS** (ESI) m/z: $[M+H]^+$ calculated for $C_{14}H_{10}N_4O_3$: 283.0753; found: 283.0754.

3-(2-(4-Chlorophenyl)hydrazineylidene)indolin-2-one (5c)

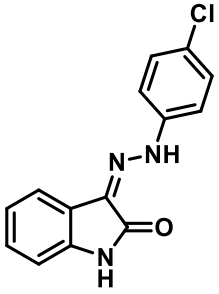

88% yield; white solid; m.p. 255-256°C; **^{1}H NMR** (500 MHz, DMSO-d_6) δ 12.70 (s, 1H), 11.05 (s, 1H), 7.55 (d, *J* = 7.5 Hz, 1H), 7.47 (m, *J* = 8.8 Hz, 2H), 7.41 (d, *J* = 8.8 Hz, 2H), 7.26 (td, *J* = 7.7Hz, 1H), 7.06 (td, *J* = 7.5 Hz, 1H), 6.93 (d, *J* = 7.8 Hz, 1H). **^{13}C NMR** (126 MHz, DMSO-d_6) δ 163.52, 142.09, 140.53, 129.75, 129.30, 128.86, 126.81, 122.42, 121.48, 119.30, 116.20, 111.05. **HRMS** (ESI) m/z: $[M+H]^+$ calculated for $C_{14}H_{10}ClN_3O$: 272.0512; found: 272.0513.

3-(2-(4-Bromophenyl)hydrazineylidene)indolin-2-one (5d)

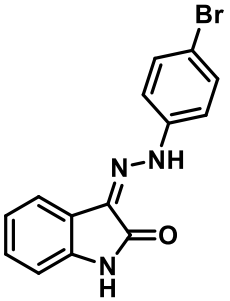

89% yield; yellowish solid; m.p. 259-260ºC; **^{1}H NMR** (500 MHz, DMSO-d_6) δ 12.71 (s, 1H), 11.05 (s, 1H), 7.56 (d, *J* = 7.4 Hz, 1H), 7.47 (d, *J* = 8.8 Hz, 2H), 7.41 (m, *J* = 9.1 Hz, 2H), 7.26 (m, *J* = 7.7 Hz, 1H), 7.06 (m, *J* = 7.5 Hz, 1H), 6.93 (d, *J* = 7.8 Hz, 1H). **^{13}C NMR** (126 MHz, DMSO-d_6) δ 163.51, 142.11, 140.54, 129.75, 129.30, 128.86, 126.81, 122.41, 121.49, 119.30, 116.20, 111.05. **HRMS** (ESI) m/z: $[M+H]^+$ calculated for $C_{14}H_{10}BrN_3O$: 316.0007; found: 316.0009.

3-(2-(4-Fluorophenyl)hydrazineylidene)indolin-2-one (5e)

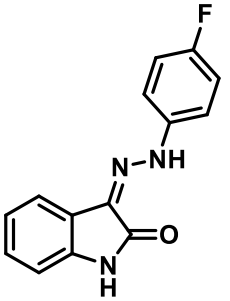

85% yield; white solid; m.p. 248-249ºC; **^{1}H NMR** (500 MHz, DMSO-d_6) δ 12.72 (s, 1H), 11.01 (s, 1H), 7.55 (d, *J* = 7.2 Hz, 1H), 7.51 – 7.46 (m, 2H), 7.27 – 7.20 (m, 3H), 7.06 (td, *J* = 7.5 Hz, 1H), 6.93 (d, *J* = 7.8 Hz, 1H). **^{13}C NMR** (126 MHz, DMSO-d_6) δ 163.53, 140.30, 139.71, 128.97, 122.32, 121.65, 119.08, 116.66, 116.48, 116.16, 116.09, 110.96. **^{19}F** NMR (471 MHz, DMSO-d6) δ -120.75. **HRMS** (ESI) m/z: $[M+H]^+$ calculated for $C_{14}H_{10}FN_3O$: 256.0808; found: 256.0809.

3-(2-(2-Chlorophenyl)hydrazineylidene)indolin-2-one (5f)

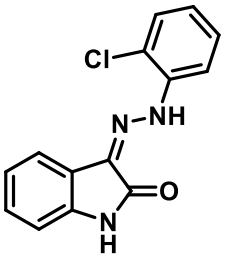

86% yield; white solid; m.p. 257-258ºC; **^{1}H NMR** (500 MHz, DMSO-d_6) δ 13.11 (s, 1H), 11.17 (s, 1H), 7.82 (m, *J* = 8.2 Hz, 1H), 7.61 (m, *J* = 7.5 Hz, 1H), 7.51 (m, *J* = 8.0 Hz, 1H), 7.45 – 7.40 (m, 1H), 7.31 (m, *J* = 7.7 Hz, 1H), 7.11 – 7.04 (m, 2H), 6.96 (d, *J* = 7.8 Hz, 1H). **^{13}C NMR** (126 MHz, DMSO-d_6) δ 163.83, 140.96, 139.25, 130.94, 130.09, 129.87, 129.06, 123.76,

122.57, 121.03, 119.71, 118.64, 114.60, 111.26. **HRMS** (ESI) m/z: $[M+H]^+$ calculated for $C_{14}H_{10}ClN_3O$: 272.0512; found: 272.0514.

3-(2-(2-Bromophenyl)hydrazineylidene)indolin-2-one (5g)

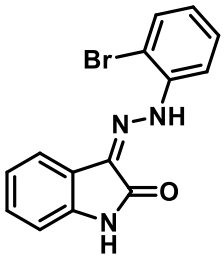

86% yield; yellowish solid; m.p. 264-265°C; **^{1}H NMR** (500 MHz, DMSO-d_6) δ 13.11 (s, 1H), 11.17 (s, 1H), 7.82 (m, *J* = 8.2 Hz, 1H), 7.61 (d, *J* = 7.1 Hz, 1H), 7.51 (m, *J* = 8.0Hz, 1H), 7.45 – 7.40 (m, 1H), 7.31 (m, *J* = 7.7 Hz, 1H), 7.12 – 7.05 (m, 2H), 6.96 (d, *J* = 7.8 Hz, 1H). **^{13}C NMR** (126 MHz, DMSO-d_6) δ 163.84, 140.97, 139.27, 130.95, 130.10, 129.88, 129.08, 123.78, 122.58, 121.04, 119.72, 118.65, 114.61, 111.27. **HRMS** (ESI) m/z: $[M+H]^+$ calculated for $C_{14}H_{10}BrN_3O$ 316.0007; found: 316.0008.

3-(2-(2,4-Dichlorophenyl)hydrazineylidene)indolin-2-one (5h)

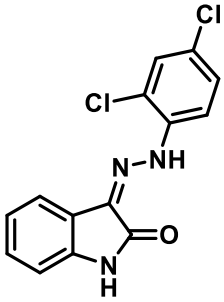

83% yield; white solid; m.p. 248-249°C; **^{1}H NMR** (500 MHz, DMSO-d_6) δ 13.09 (s, 1H), 11.20 (s, 1H), 7.80 (d, *J* = 8.9 Hz, 1H), 7.69 (d, *J* = 7.3 Hz, 1H), 7.61 (d, *J* = 7.2 Hz, 1H), 7.49 (m, *J* = 8.8 Hz, 1H), 7.34 – 7.29 (m, 1H), 7.09 (m, *J* = 7.6 Hz, 1H), 6.96 (d, *J* = 7.8 Hz, 1H). **^{13}C NMR** (126 MHz, DMSO-d_6) δ 163.84, 141.17, 138.52, 131.61, 130.16, 129.43, 129.19, 126.50, 122.66, 120.85, 119.90, 119.19, 115.68, 111.34. **HRMS** (ESI) m/z: $[M+H]^+$ calculated for $C_{14}H_9Cl_2N_3O$: 306.0123; found: 306.0125.

3-(2-(2,4-Dibromophenyl)hydrazineylidene)indolin-2-one (5i)

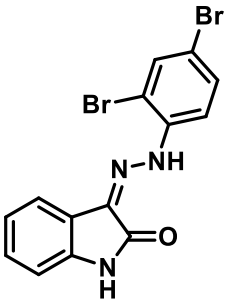

82% yield; white solid; m.p. 237-238°C; **^{1}H NMR** (500 MHz, DMSO-d_6) δ 13.09 (s, 1H), 11.20 (s, 1H), 7.80 (d, *J* = 8.9 Hz, 1H), 7.69 (d, *J* = 2.3 Hz, 1H), 7.61 (d, *J* = 7.4 Hz, 1H), 7.49 (m, *J* = 8.8 Hz, 1H), 7.32 (m, *J* = 7.7 Hz, 1H), 7.09 (m, *J* = 7.5 Hz, 1H), 6.96 (d, *J* = 7.8 Hz, 1H). **^{13}C NMR** (126 MHz, DMSO-d_6) δ 163.84, 141.17, 138.53, 131.61, 130.17, 129.43, 129.19, 126.51, 122.66, 120.85, 119.90, 119.20, 115.69, 111.35. **HRMS** (ESI) m/z: $[M+H]^+$ calculated for $C_{14}H_9Br_2N_3O$: 393.9112; found: 393.9114.

3-(2-(3,4-Dichlorophenyl)hydrazineylidene)indolin-2-one (5j)

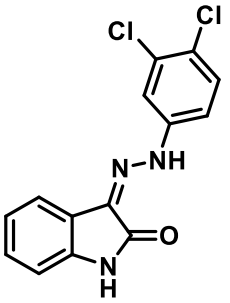

86% yield; white solid; m.p. 238-239°C; **^{1}H NMR** (500 MHz, DMSO-d_6) δ 13.09 (s, 1H), 11.20 (s, 1H), 7.80 (d, *J* = 8.9 Hz, 1H), 7.69 (d, *J* = 2.3 Hz, 1H), 7.61 (d, *J* = 7.4 Hz, 1H), 7.49 (m, *J* = 8.8 Hz, 1H), 7.32 (m, *J* = 7.7 Hz, 1H), 7.09 (m, *J* = 7.5 Hz, 1H), 6.96 (d, *J* = 7.8 Hz, 1H). **^{13}C NMR** (126 MHz, DMSO-d_6) δ 163.84, 141.17, 138.53, 131.61, 130.17, 129.43, 129.19, 126.51, 122.66, 120.85, 119.90, 119.20, 115.69, 111.35. **HRMS** (ESI) m/z: $[M+H]^+$ calculated for $C_{14}H_9Cl_2N_3O$: 306.0123; found: 306.0124.

3-(2-(2,4-Dimethylphenyl)hydrazineylidene)indolin-2-one (5k)

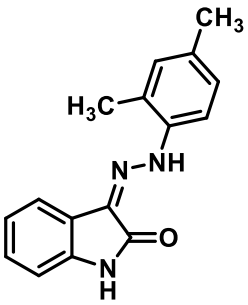

85% yield; reddish solid; m.p. 229-230°C; **^{1}H NMR** (500 MHz, DMSO-d_6) δ 12.95 (s, 1H), 11.07 (s, 1H), 7.61 – 7.55 (m, 2H), 7.25 (m, *J* = 7.7 Hz, 1H), 7.12 – 7.04 (m, 3H), 6.95 (d, *J* = 7.8 Hz, 1H), 2.26 (d, *J* = 5.2 Hz, 6H). **^{13}C NMR** (126 MHz, DMSO-d_6) δ 164.05, 140.01, 138.51, 132.10, 131.78, 128.75, 128.33, 128.28, 122.89, 122.34,

121.52, 118.95, 112.89, 111.05, 20.83, 16.77. **HRMS** (ESI) m/z: $[M+H]^+$ calculated for $C_{16}H_{15}N_3O$: 266.1215; found: 266.1216.

3-(2-(4-Methoxyphenyl)hydrazineylidene)indolin-2-one (5l)

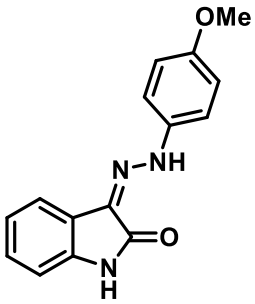

86% yield; brick red solid; m.p. 227-229°C; **^{1}H NMR** (500 MHz, DMSO-d_6) δ 12.78 (s, 1H), 10.96 (s, 1H), 7.53 (d, *J* = 7.4 Hz, 1H), 7.40 (d, *J* = 9.0 Hz, 2H), 7.22 (t, *J* = 8.3 Hz, 1H), 7.04 (m, *J* = 9.3 Hz, 1H), 6.97 (d, *J* = 9.0 Hz, 2H), 6.92 (d, *J* = 7.8 Hz, 1H), 3.76 (s, 3H). **^{13}C NMR** (126 MHz, DMSO-d_6) δ 163.66, 156.03, 139.81, 136.65, 128.39, 126.82, 122.18, 121.86, 118.70, 115.93, 115.28, 110.86, 55.81. **HRMS** (ESI) m/z: $[M+H]^+$ calculated for $C_{15}H_{13}N_3O_2$: 268.1008; found: 268.1009.

3-(2-(3,4-Dimethylphenyl)hydrazineylidene)indolin-2-one (5m)

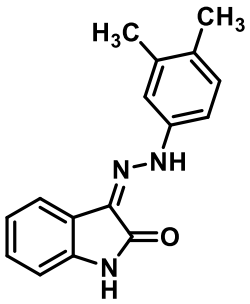

86% yield; white solid; m.p. 238-239°C; **^{1}H NMR** (500 MHz, DMSO-d_6) δ 12.95 (s, 1H), 11.07 (s, 1H), 7.60 – 7.55 (m, 2H), 7.25 (m, *J* = 7.7 Hz, 1H), 7.09 (m, *J* = 7.1 Hz, 1H), 7.06 (m, *J* = 7.6 Hz, 2H), 6.95 (d, *J* = 7.8 Hz, 1H), 2.26 (d, *J* = 5.2 Hz, 6H). **^{13}C NMR** (126 MHz, DMSO-d_6) δ 164.05, 140.01, 138.51, 132.10, 131.78, 128.75, 128.33, 128.28, 122.89, 122.34, 121.52, 118.95, 112.89, 111.05, 20.83, 16.78. **HRMS** (ESI) m/z: $[M+H]^+$ calculated for $C_{16}H_{15}N_3O$: 266.1215; found: 266.1217.

3-(2-(4-Isopropylphenyl)hydrazineylidene)indolin-2-one (5n)

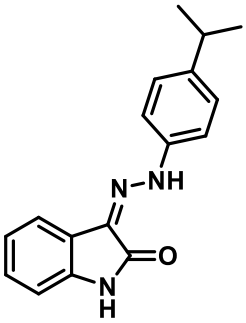

88% yield; white solid; m.p. 228-229°C; **^{1}H NMR** (500 MHz, DMSO-d_6) δ 12.78 (s, 1H), 11.13 (s, 1H), 7.55 (d, *J* = 7.1 Hz, 1H), 7.41 (d, *J* = 8.6 Hz, 2H), 7.26 (m, *J* = 8.6 Hz, 4H), 6.93 (d, *J* = 8.3 Hz, 1H), 2.91 – 2.85 (m, 1H), 1.21 (d, *J* = 6.9 Hz, 6H). **^{13}C NMR** (126 MHz, DMSO-d_6) δ 163.47, 144.23, 140.71, 138.56, 127.95, 127.74, 126.51, 126.30, 123.54, 118.43, 115.02, 112.33, 33.34, 24.42. **HRMS** (ESI) m/z: $[M+H]^+$ calculated for $C_{16}H_{15}N_3O$: 279.1372; found: 279.1374.

3-(2-Mesitylhydrazineylidene)indolin-2-one (5o)

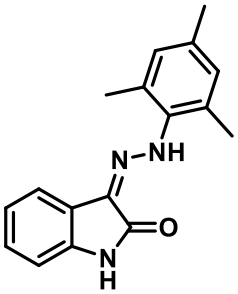

82% yield; white solid; m.p. 231-232 °C; **^{1}H NMR** (500 MHz, DMSO-d_6) δ 12.76 (s, 1H), 11.02 (s, 1H), 7.24 (m, J = 8.4 Hz, 1H), 7.06 – 7.01 (m, 1H), 6.95 – 6.90 (m, 3H), 2.36 (s, 6H), 2.24 (s, 3H). **^{13}C NMR** (126 MHz, DMSO-d_6) δ 163.51, 138.06, 136.50, 134.15, 130.42, 128.50, 127.54, 126.43, 125.87, 123.72, 117.80, 112.33, 20.82, 19.37. **HRMS** (ESI) m/z: $[M+H]^+$ calculated for $C_{17}H_{17}N_3O$: 279.1372; found: 279.1375.

3-(2-(Benzo[d]thiazol-2-yl)hydrazineylidene)indolin-2-one (5p)

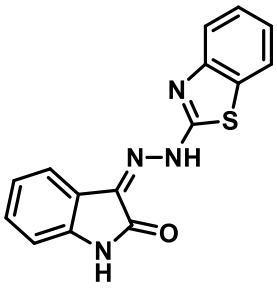

83% yield; brick red solid; m.p. 270-272°C; **^{1}H NMR** (500 MHz, DMSO-d_6) δ 12.13 (s, 1H), 11.04 (s, 1H), 7.59 (m, *J* = 7.7 Hz, 2H), 7.51 (m, *J* = 7.4 Hz, 2H), 7.07 (m, *J* = 7.4 Hz, 2H), 6.91 (m, *J* = 7.9 Hz, 2H). **^{13}C NMR** (126 MHz, DMSO-d_6) δ 184.86, 159.83, 151.19, 138.84, 136.28, 127.58, 125.16, 123.23, 118.30, 112.67. **HRMS** (ESI) m/z: $[M+H]^+$ calculated for $C_{15}H_{11}N_4OS$: 295.0648; found: 295.0644.

1-Benzylidene-2-phenylhydrazine (6a)

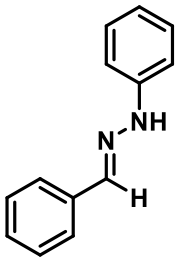

86% yield; white solid; m.p. 210-212°C; **^{1}H NMR** (500 MHz, DMSO-d_6) δ 10.34 (s, 1H), 7.86 (s, 1H), 7.67 – 7.63 (m, 2H), 7.39 (t, *J* = 7.6 Hz, 2H), 7.29 (t, *J* = 7.3 Hz, 1H), 7.22 (m, *J* =7.4 Hz, 2H), 7.08 (d, *J* = 1.0 Hz, 2H), 6.75 (t, *J* = 7.3 Hz, 1H). **^{13}C NMR** (126 MHz, DMSO-d_6) δ 145.75, 136.87, 136.30, 129.59, 129.12, 128.38, 126.08, 119.21, 112.44. **HRMS** (ESI) m/z: $[M+H]^+$ calculated for $C_{13}H_{12}N_2$: 197.1000; found: 197.1002.

1-(3-Chlorobenzylidene)-2-phenylhydrazine (6b)

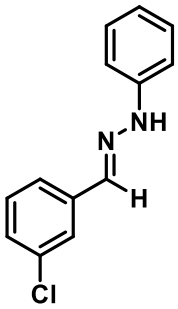

90% yield; light brown; m.p. 215-216°C; **^{1}H NMR** (500 MHz, DMSO-d_6) δ 10.52 (s, 1H), 7.83 (s, 1H), 7.70 (s, 1H), 7.60 (d, *J* = 7.7 Hz, 1H), 7.41 (t, *J* = 7.8 Hz, 1H), 7.33 (d, *J* = 5.8 Hz, 1H), 7.26 – 7.21 (m, 2H), 7.09 (d, *J* = 7.5 Hz, 2H), 6.78 (t, *J* = 7.3 Hz, 1H). **^{13}C NMR** (126 MHz, DMSO-d_6) δ 145.42, 138.65, 135.03, 134.01, 130.97, 129.63, 127.87, 124.68, 112.63. **HRMS** (ESI) m/z: $[M+H]^+$ calculated for $C_{13}H_{11}ClN_2$: 231.0611; found: 231.0613.

1-(2,4-Dichlorobenzylidene)-2-phenylhydrazine (6c)

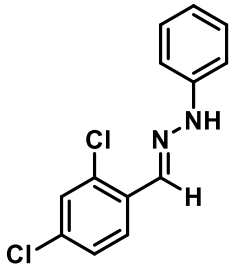

87% yield; cream solid; m.p. 219-221°C; **^{1}H NMR** (500 MHz, DMSO-d_6) δ 10.80 (s, 1H), 8.14 (s, 1H), 8.02 (d, *J* = 8.6 Hz, 1H), 7.62 (d, *J* = 2.1 Hz, 1H), 7.44 (d, *J* = 8.6 Hz, 1H), 7.27 – 7.23 (m, 2H), 7.10 (d, *J* = 7.6 Hz, 2H), 6.81 (t, *J* = 7.3 Hz, 1H). **^{13}C NMR** (126 MHz, DMSO-d_6) δ 145.08, 132.09, 131.24, 129.69, 129.56, 128.18, 127.40, 120.02, 112.74. **HRMS** (ESI) m/z: $[M+H]^+$ calculated for $C_{13}H_{10}Cl_2N_2$: 265.0221; found: 265.0222.

1-(3,4-Dichlorobenzylidene)-2-phenylhydrazine (6d)

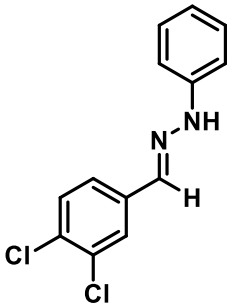

87% yield; white solid; m.p. 216-218°C; **^{1}H NMR** (500 MHz, DMSO-d_6) δ 10.81 (s, 1H), 8.14 (s, 1H), 8.02 (d, *J* = 8.6 Hz, 1H), 7.63 (d, *J* = 7.1 Hz, 1H), 7.44 (m, *J* = 8.6 Hz, 1H), 7.27 – 7.21 (m, 2H), 7.10 (d, *J* = 7.6 Hz, 2H), 6.81 (t, *J* = 7.3 Hz, 1H). **^{13}C NMR** (126 MHz, DMSO-d_6) δ 145.07, 132.88, 132.54, 132.09, 131.23, 129.70, 129.57, 128.20, 127.40, 120.02, 112.73. **HRMS** (ESI) m/z: $[M+H]^+$ calculated for $C_{13}H_{10}Cl_2N_2$: 265.0221; found: 265.0223.

1-(3-Bromobenzylidene)-2-phenylhydrazine (6e)

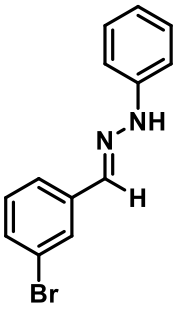

92% yield; white solid; m.p. 213-215°C; **^{1}H NMR** (500 MHz, DMSO-d_6) δ 10.53 (s, 1H), 7.83 (s, 1H), 7.71 – 7.69 (m, 1H), 7.60 (d, *J* = 7.8 Hz, 1H), 7.41 (t, *J* = 7.8 Hz, 1H), 7.33 (m, *J* = 7.9 Hz, 1H), 7.26 – 7.21 (m, 2H), 7.09 (m, *J* = 8.6 Hz, 2H), 6.78 (m, *J* = 13.5 Hz, 1H). **^{13}C NMR** (126 MHz, DMSO-d_6) δ 145.40, 138.63, 135.01, 133.99, 130.96, 129.62, 127.86, 125.24, 124.67, 119.59, 112.61. **HRMS** (ESI) m/z: $[M+H]^+$ calculated for $C_{13}H_{11}BrN_2$: 275.0106; found: 275.0107.

1-(2,4-Dibromobenzylidene)-2-phenylhydrazine (6f)

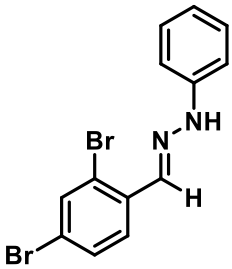

88% yield; white solid; m.p. 217-219°C; **^{1}H NMR** (500 MHz, DMSO-d_6) δ 10.81 (s, 1H), 8.14 (s, 1H), 8.02 (d, *J* = 8.6 Hz, 1H), 7.63 (d, *J* = 8.1 Hz, 1H), 7.44 (m, *J* = 8.6 Hz, 1H), 7.25 (m, *J* = 7.4 Hz, 2H), 7.12 – 7.08 (m, 2H), 6.81 (t, *J* = 7.3 Hz, 1H). **^{13}C NMR** (126 MHz, DMSO-d_6)

δ 145.05, 132.88, 132.53, 132.08, 131.22, 129.68, 129.56, 128.18, 127.39, 120.02, 112.72. **HRMS** (ESI) m/z: $[M+H]^+$ calculated for $C_{13}H_{10}Br_2N_2$: 352.9211; found: 352.9210.

1-(4-Nitrobenzylidene)-2-phenylhydrazine (6g)

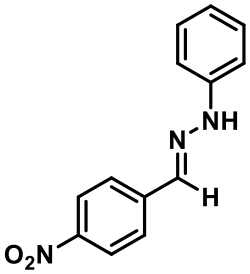

93% yield; reddish brown solid; m.p. 205-207°C; **^{1}H NMR** (500 MHz, DMSO-d_6) δ 11.38 (s, 1H), 8.28 – 8.23 (m, 2H), 8.05 (s, 1H), 7.96 (d, *J* = 9.4 Hz, 2H), 7.68 (d, *J* = 8.9 Hz, 2H), 7.25 (d, *J* = 8.7 Hz, 2H). **^{13}C NMR** (126 MHz, DMSO-d_6) δ 148.46, 147.29, 142.20, 137.68, 134.24, 127.31, 124.40, 120.32, 113.08. **HRMS** (ESI) m/z: $[M+H]^+$ calculated for $C_{13}H_{11}N_3O_2$: 242.0851; found: 242.0853.

1-(3-Nitrobenzylidene)-2-phenylhydrazine (6h)

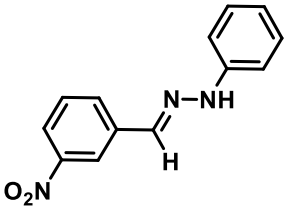

91% yield; red solid; m.p. 208-209°C; **^{1}H NMR** (500 MHz, DMSO-d_6) δ 10.69 (s, 1H), 8.45 – 8.43 (m, 1H), 8.12 – 8.08 (m, 2H), 7.97 (s, 1H), 7.66 (t, *J* = 8.0 Hz, 1H), 7.26 (t, *J* = 7.8 Hz, 2H), 7.13 (d, *J* = 7.8 Hz, 2H), 6.81 (d, *J* = 7.2 Hz, 1H). **^{13}C NMR** (126 MHz, DMSO-d_6) δ 148.78, 145.21, 138.33, 134.21, 130.60, 129.67, 122.41, 119.96, 119.90, 112.74. **HRMS** (ESI) m/z: $[M+H]^+$ calculated for $C_{13}H_{11}N_3O_2$: 242.0851; found: 242.0853.

1-(3,4-Dimethoxybenzylidene)-2-phenylhydrazine (6i)

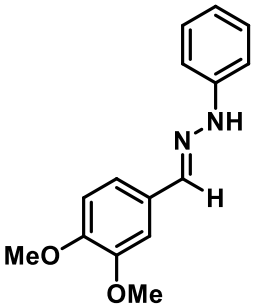

85% yield; white solid; m.p. 198-200°C; **^{1}H NMR** (500 MHz, DMSO-d_6) δ 9.88 (s, 1H), 7.92 – 7.86 (m, 4H), 7.16 – 7.11 (m, 3H), 7.02 (d, *J* = 9.0 Hz, 1H), 3.85 (d, *J* = 21.8 Hz, 6H).**^{13}C NMR** (126 MHz, DMSO-d_6) δ 167.48, 164.70, 163.30, 132.27, 131.80, 130.14, 123.48, 114.98,

114.27, 56.15, 55.89. **HRMS** (ESI) m/z: $[M+H]^+$ calculated for $C_{15}H_{16}N_2O_2$: 257.1212; found: 257.1215.

1-(4-Methoxybenzylidene)-2-phenylhydrazine (6j)

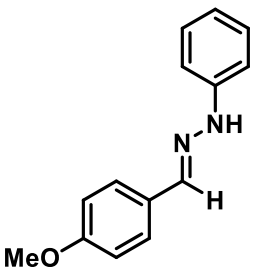

86% yield; cream solid; m.p. 201-203°C; **^{1}H NMR** (500 MHz, DMSO-d_6) δ 10.81 (s, 1H), 7.93 (s, 1H), 7.65 (d, *J* = 6.8 Hz, 2H), 7.61 (s, 2H), 7.13 (s, 2H), 7.00 (d, *J* = 4.7 Hz, 2H), 3.80 (s, 3H). **^{13}C NMR** (126 MHz, DMSO-d_6) δ 160.35, 149.18, 140.65, 133.51, 127.95, 120.79, 114.69, 112.27, 55.78. **HRMS** (ESI) m/z: $[M+H]^+$ calculated for $C_{14}H_{14}N_2O$: 227.1106; found: 227.1108.

4-(2-(4-Methoxybenzylidene)hydrazineyl)benzonitrile (6k)

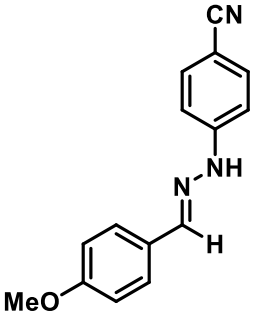

89% yield; whitish brown solid; m.p. 231-232°C; **^{1}H NMR** (500 MHz, DMSO-d_6) δ 10.81 (s, 1H), 7.93 (s, 1H), 7.66 – 7.64 (m, 2H), 7.60 (d, *J* = 9.0 Hz, 2H), 7.12 (d, *J* = 8.6 Hz, 2H), 7.00 – 6.97 (m, 2H), 3.80 (s, 3H). **^{13}C NMR** (126 MHz, DMSO-d_6) δ 160.45, 149.26, 140.65, 134.10, 128.21, 128.09, 120.67, 114.73, 112.34, 99.23, 55.72. **HRMS** (ESI) m/z: $[M+H]^+$ calculated for $C_{15}H_{13}N_3O$: 252.1059; found: 252.1057.

4-(2-(4-Nitrobenzylidene)hydrazineyl)benzonitrile (6l)

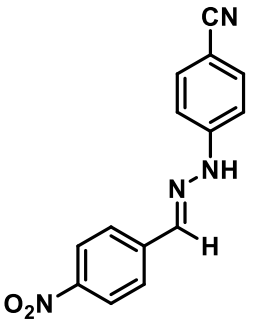

90% yield; dark orange solid; m.p. 224-225°C; **^{1}H NMR** (500 MHz, DMSO-d_6) δ 11.38 (s, 1H), 8.25 (d, *J* = 8.9 Hz, 2H), 8.05 (s, 1H), 7.96 (d, *J* = 8.9 Hz, 2H), 7.68 (d, *J* = 8.9 Hz, 2H), 7.25 (d, *J* = 8.7 Hz, 2H). **^{13}C NMR** (126 MHz, DMSO-d_6) δ 148.46, 147.23, 142.08, 137.83,

134.24, 127.31, 124.53, 120.32, 113.20, 101.07. **HRMS** (ESI) m/z: $[M+H]^+$ calculated for $C_{14}H_{10}N_4O_2$: 267.0804; found: 267.0807.

1-Benzylidene-2-(2-chlorophenyl)hydrazine (6m)

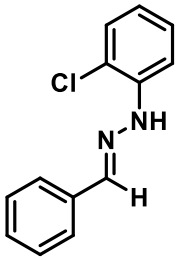

85% yield; white solid; m.p. 213-215°C; **^{1}H NMR** (500 MHz, DMSO-d_6) δ 9.90 (s, 1H), 8.30 (s, 1H), 7.68 (d, *J* = 7.2 Hz, 2H), 7.58 (d, *J* = 8.2 Hz, 1H), 7.42 (t, *J* = 7.5 Hz, 2H), 7.34 (t, *J* = 6.6 Hz, 2H), 7.27 (t, *J* = 8.2 Hz, 1H), 6.82 – 6.78 (m, 1H). **^{13}C NMR** (126 MHz, DMSO-d_6) δ 141.88, 140.85, 135.91, 129.83, 129.21, 129.03, 128.53, 126.50, 120.10, 116.65, 114.52. **HRMS** (ESI) m/z: $[M+H]^+$ calculated for $C_{13}H_{11}ClN_2$: 231.0611; found: 231.0614.

1-Benzylidene-2-(4-chlorophenyl)hydrazine (6n)

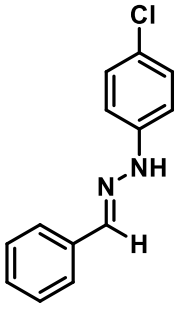

86% yield; white solid; m.p. 217-218°C; **^{1}H NMR** (500 MHz, DMSO-d_6) δ 10.47 (s, 1H), 7.88 (s, 1H), 7.67 – 7.64 (m, 2H), 7.40 (m, *J* = 7.6 Hz, 2H), 7.32 (m, *J* = 8.1 Hz, 1H), 7.27 – 7.23 (m, 2H), 7.10 – 7.06 (m, 2H). **^{13}C NMR** (126 MHz, DMSO-d_6) δ 144.70, 137.79, 136.04, 129.39, 129.13, 128.64, 126.23, 122.43, 113.88. **HRMS** (ESI) m/z: $[M+H]^+$ calculated for $C_{13}H_{11}ClN_2$: 231.0611; found: 231.0608.

1-Benzylidene-2-(2,4-dichlorophenyl)hydrazine (6o)

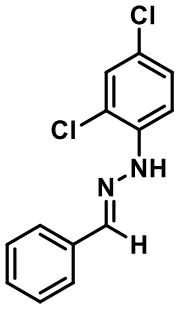

84% yield; white solid; m.p. 223-224°C; **^{1}H NMR** (500 MHz, DMSO-d_6) δ 10.05 (s, 1H), 8.31 (s, 1H), 7.70 – 7.66 (m, 2H), 7.57 (d, *J* = 8.9 Hz, 1H), 7.47 (d, *J* = 8.3 Hz, 1H), 7.42 (t, *J* = 7.5 Hz, 2H), 7.36 (d, *J* = 7.4 Hz, 1H), 7.33 – 7.30 (m, 1H). **^{13}C NMR** (126 MHz, DMSO-d_6) δ 141.61, 141.11,

135.68, 129.24, 129.22, 129.06, 128.54, 126.62, 122.67, 117.11, 115.52. **HRMS** (ESI) m/z: $[M+H]^+$ calculated for $C_{13}H_{10}Cl_2N_2$: 265.0221; found: 265.0224.

1-Benzylidene-2-(2-bromophenyl)hydrazine (6p)

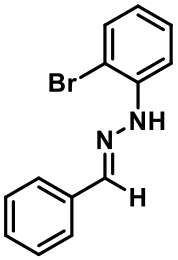

86% yield; white solid; m.p. 218-219°C; **^{1}H NMR** (500 MHz, DMSO-d_6) δ 9.89 (s, 1H), 8.30 (s, 1H), 7.68 (d, *J* = 9.3 Hz, 2H), 7.60 – 7.57 (m, 1H), 7.42 (t, *J* = 7.5 Hz, 2H), 7.34 (t, *J* = 8.5 Hz, 2H), 7.27 (t, *J* = 7.7 Hz, 1H), 6.83 – 6.77 (m, 1H). **^{13}C NMR** (126 MHz, DMSO-d_6) δ 141.95, 140.85, 135.91, 129.75, 129.28, 129.03, 128.53, 126.50, 120.10, 116.75, 114.64. **HRMS** (ESI) m/z: $[M+H]^+$ calculated for $C_{13}H_{11}BrN_2$: 275.0106; found: 275.0108.

1-Benzylidene-2-(4-bromophenyl)hydrazine (6q)

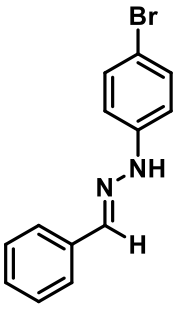

89% yield; white solid; m.p. 227-228°C; **^{1}H NMR** (500 MHz, DMSO-d_6) δ 10.47 (s, 1H), 7.88 (s, 1H), 7.68 – 7.63 (m, 2H), 7.39 (t, *J* = 6.8 Hz, 2H), 7.33 – 7.28 (m, 1H), 7.25 (d, *J* = 8.9 Hz, 2H), 7.07 (d, *J* = 8.9 Hz, 2H). **^{13}C NMR** (126 MHz, DMSO-d_6) δ 144.68, 137.79, 136.04, 129.39, 129.06, 128.55, 126.23, 122.36, 113.95. **HRMS** (ESI) m/z: $[M+H]^+$ calculated for $C_{13}H_{11}BrN_2$: 275.0106; found: 275.0107.

1-Benzylidene-2-(2,4-dibromophenyl)hydrazine (6r)

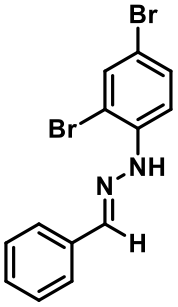

87% yield; white solid; m.p. 228-229°C; **^{1}H NMR** (500 MHz, DMSO-d_6) δ 10.05 (s, 1H), 8.31 (s, 1H), 7.68 (d, *J* = 8.5 Hz, 2H), 7.57 (d, *J* = 8.9 Hz, 1H), 7.47 (s, 1H), 7.44 – 7.40 (m, 2H), 7.37 – 7.33 (m, 1H), 7.31 (d, *J* = 8.9 Hz, 1H). **^{13}C NMR** (126 MHz, DMSO-d_6) δ 141.61, 141.11, 135.78, 129.24,

128.99, 128.45, 126.74, 122.61, 117.19, 115.52. **HRMS** (ESI) m/z: $[M+H]^+$ calculated for $C_{13}H_{10}Br_2N_2$: 352.9211; found: 352.9210.

1-Benzylidene-2-(2,4-dimethylphenyl)hydrazine (6s)

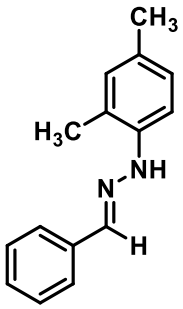

86% yield; cream solid; m.p. 216-218°C; **^{1}H NMR** (500 MHz, DMSO-d_6) δ 10.38 (d, *J* = 8.0 Hz, 1H), 7.93 (m, *J* = 8.3 Hz, 2H), 7.58 (d, *J* = 7.4 Hz, 1H), 7.54 – 7.50 (m, 2H), 7.12 (d, *J* = 3.0 Hz, 1H), 6.87 – 6.81 (m, 2H), 6.63 (d, *J* = 8.1 Hz, 1H), 2.18 (d, *J* = 11.9 Hz, 6H). **^{13}C NMR** (126 MHz, DMSO-d_6) δ 166.59, 145.01, 133.54, 132.05, 131.18, 128.95, 127.83, 127.72, 127.16, 122.63, 111.97, 20.57, 17.67. **HRMS** (ESI) m/z: $[M+H]^+$ calculated for $C_{15}H_{16}N_2$: 225.1313; found: 225.1315.

1-Benzylidene-2-(4-fluorophenyl)hydrazine (6t)

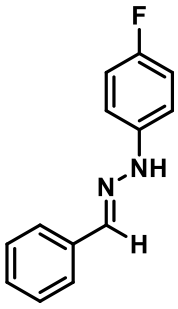

80% yield; white solid; m.p. 210-211°C; **^{1}H NMR** (500 MHz, DMSO-d_6) δ 10.47 (s, 1H), 7.88 (s, 1H), 7.68 – 7.64 (m, 2H), 7.40 (m, *J* = 7.6 Hz, 2H), 7.33 – 7.28 (m, 1H), 7.28 – 7.24 (m, 2H), 7.10 – 7.05 (m, 2H). **^{13}C NMR** (126 MHz, DMSO-d_6) δ 144.63, 137.79, 136.04, 129.45, 129.26, 128.64, 126.23, 122.43, 113.98. **^{19}F NMR** (471 MHz, DMSO-d_6) δ -121.65, -121.66. **HRMS** (ESI) m/z: $[M+H]^+$ calculated for $C_{13}H_{12}N_2F$: 215.0979; found: 215.0976.

1-(Naphthalen-1-ylmethylene)-2-phenylhydrazine (6u)

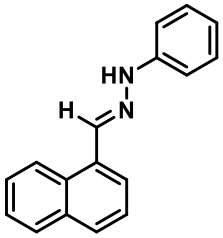

81% yield; brown solid; m.p. 79-80°C; **^{1}H NMR** (500 MHz, DMSO-d_6) δ 10.41 (s, 1H), 9.17 (d, *J* = 8.5 Hz, 2H), 8.27 (d, *J* = 8.2 Hz, 2H), 8.18 (d, *J* = 7.1 Hz, 2H), 8.07 (d, *J* = 8.2 Hz, 1H), 7.78 – 7.69 (m, 4H), 7.65 (t, *J* = 6.9 Hz, 2H). **^{13}C NMR** (126 MHz, DMSO-d_6) δ 152.30, 137.22,

135.71, 133.79, 131.34, 130.25, 129.48, 129.18, 127.38, 125.84, 124.60. **HRMS** (ESI) m/z: $[M+H]^+$ calculated for $C_{17}H_{15}N_2$: 247.1230; found: 247.1232.

1-Phenyl-2-(thiophen-2-ylmethylene)hydrazine(6v)

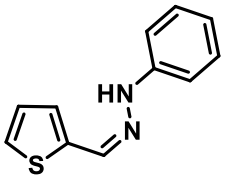

78% yield; white solid; m.p. 145-147°C; **^{1}H NMR** (500 MHz, DMSO-d_6) δ 10.30 (s, 1H), 8.06 (s, 1H), 7.46 (d, *J* = 5.0 Hz, 1H), 7.21 (s, 3H), 7.06 (m, *J* = 7.9 Hz, 1H), 6.99 (d, *J* = 7.7 Hz, 2H), 6.74 (t, *J* = 7.3 Hz, 1H). **^{13}C NMR** (126 MHz, DMSO-d_6) δ 145.52, 141.39, 132.47, 129.60, 128.05, 127.04, 126.21, 119.23, 112.34. **HRMS** (ESI) m/z: $[M+H]^+$ calculated for $C_{11}H_{11}N_2S$: 203.0637; found: 203.0639.

2-(2-Benzylidenehydrazineyl)benzo[d]thiazole (6w)

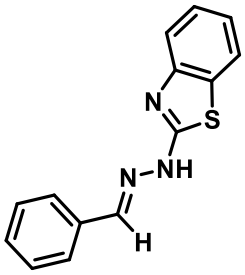

83% yield; brown solid; m.p. 190-191°C; **^{1}H NMR** (500 MHz, DMSO-d_6) δ 12.49 (s, 1H), 8.44 (s, 2H), 7.55 (d, *J* = 8.1 Hz, 2H), 7.36 (m, *J* = 7.9 Hz, 2H), 7.21 (m, *J* = 7.7 Hz, 2H), 7.15 (d, *J* = 7.9 Hz, 2H). **^{13}C NMR** (126 MHz, DMSO-d_6) δ 161.36, 151.06, 145.30, 138.70, 130.06, 128.73, 125.96, 123.54, 111.81. **HRMS** (ESI) m/z: $[M+H]^+$ calculated for $C_{14}H_{12}N_3S$: 254.0746; found: 254.0749.

2.8 Spectral Data of few compounds

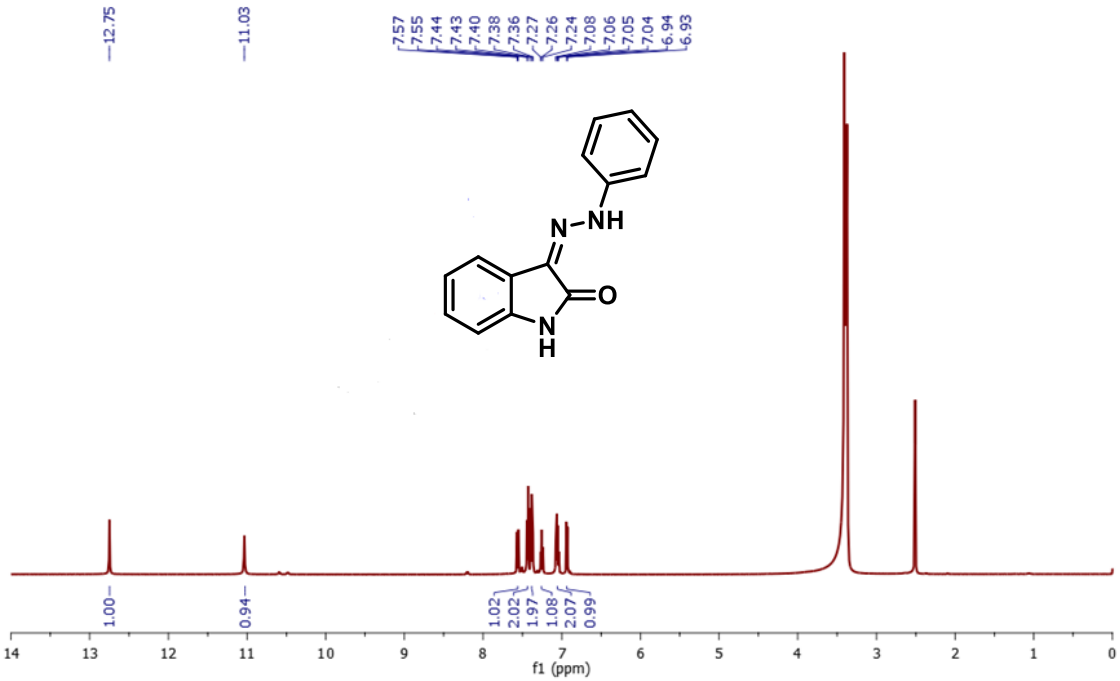

Figure 2.7 ^{1}H-NMR spectrum of **4a** (500 MHz, DMSO-d_6)

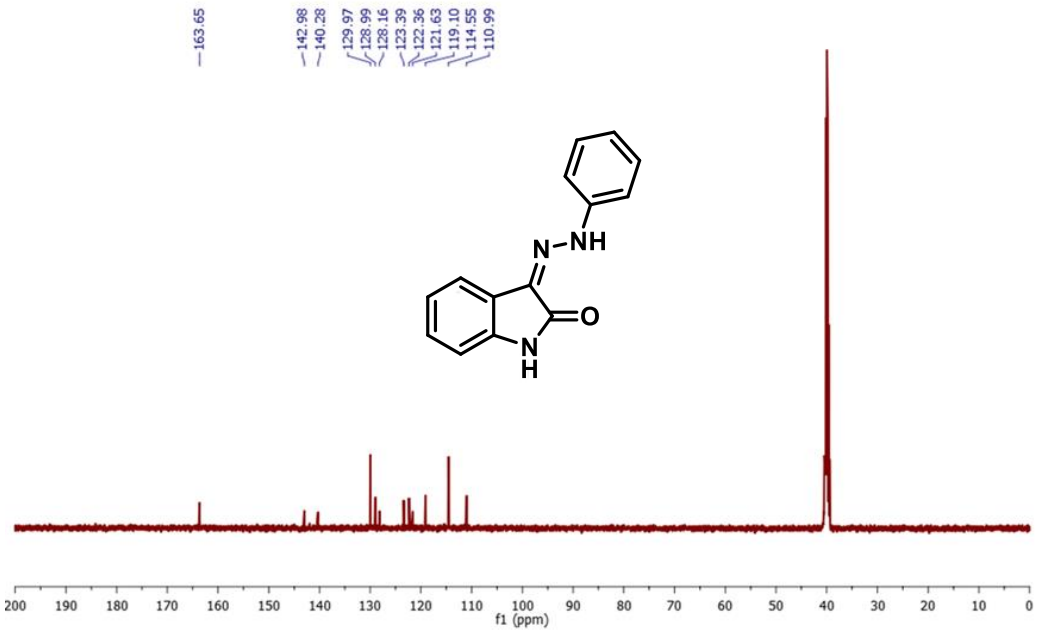

Figure 2.8 ^{13}C-NMR spectrum of **4a** (126 MHz, DMSO-d_6)

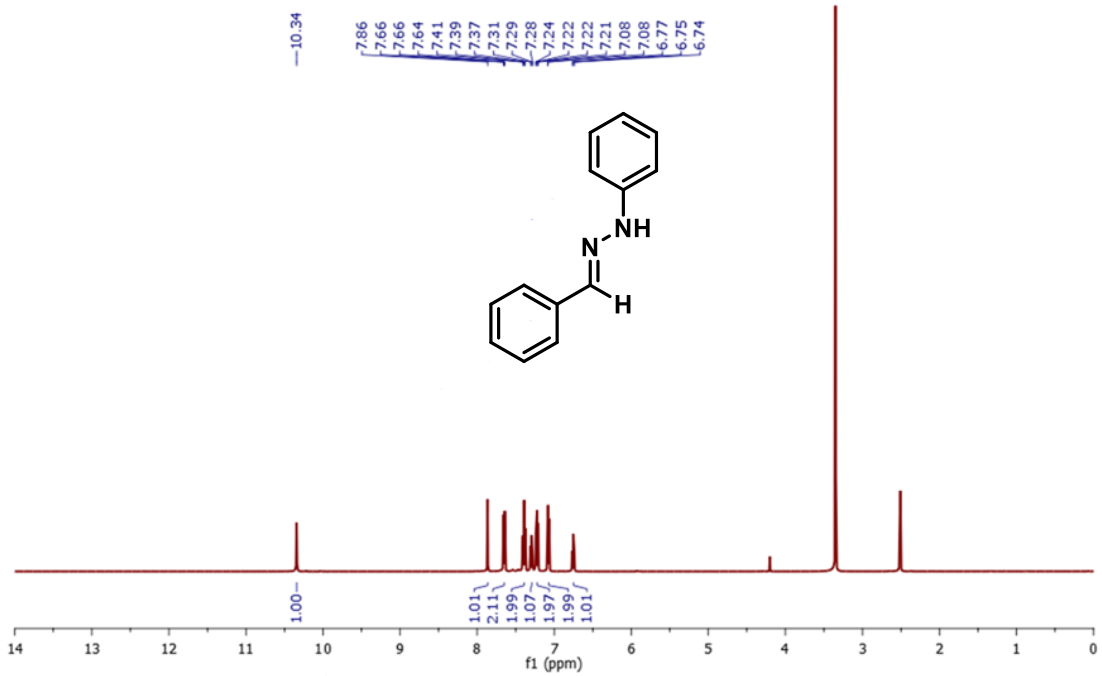

Figure 2.9 ^{1}H-NMR spectrum of **6a** (500 MHz, DMSO-d_6)

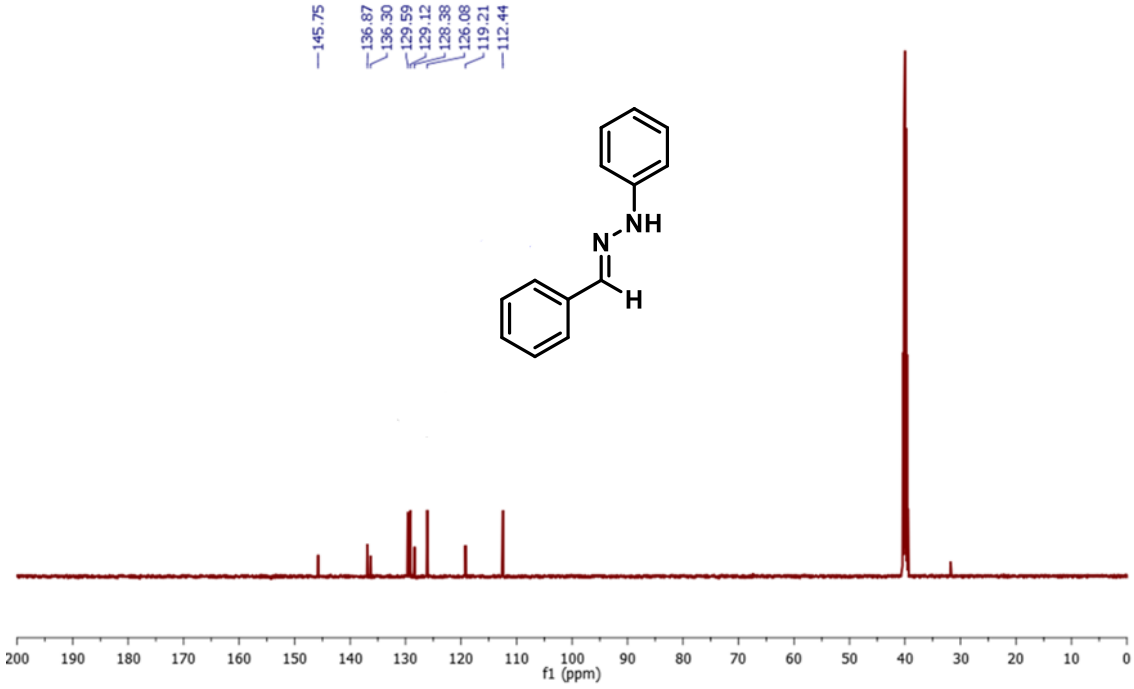

Figure 2.10 ^{13}C-NMR spectrum of **6a** (126 MHz, DMSO-d_6)

2.9 HRMS Data

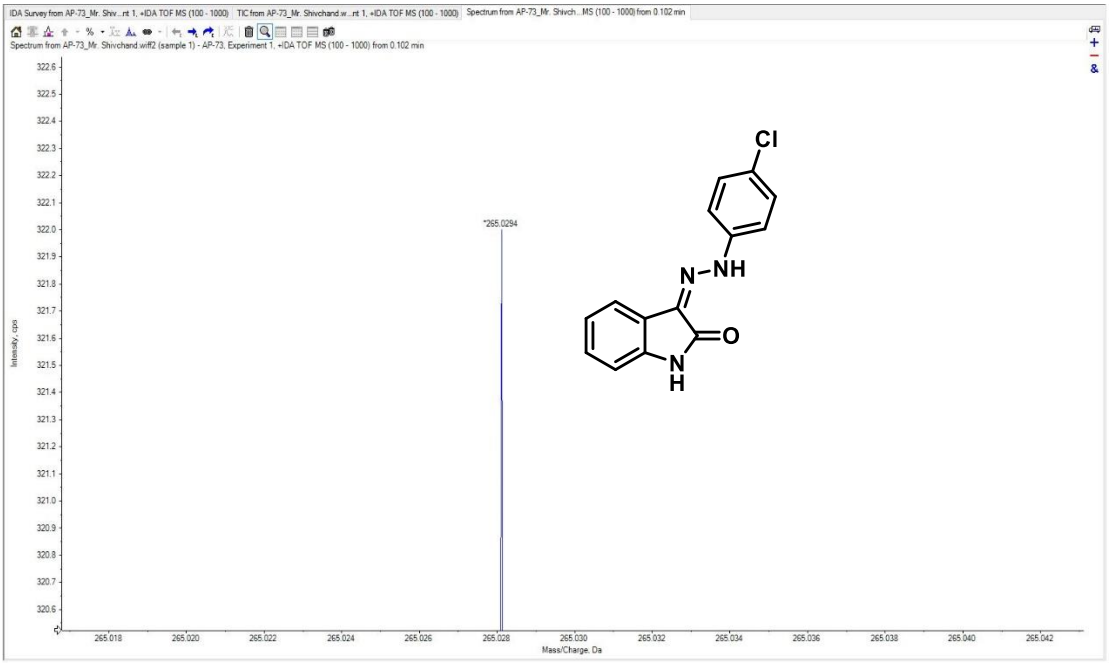

Figure 2.11 HRMS of compound **5c**

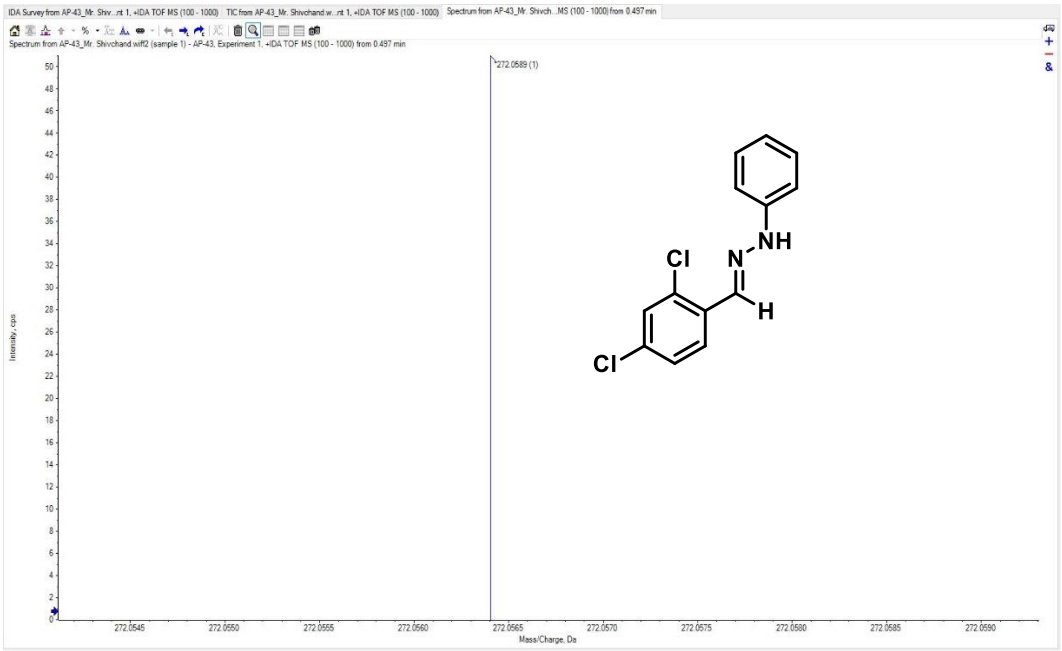

Figure 2.12 HRMS of compound **6c**

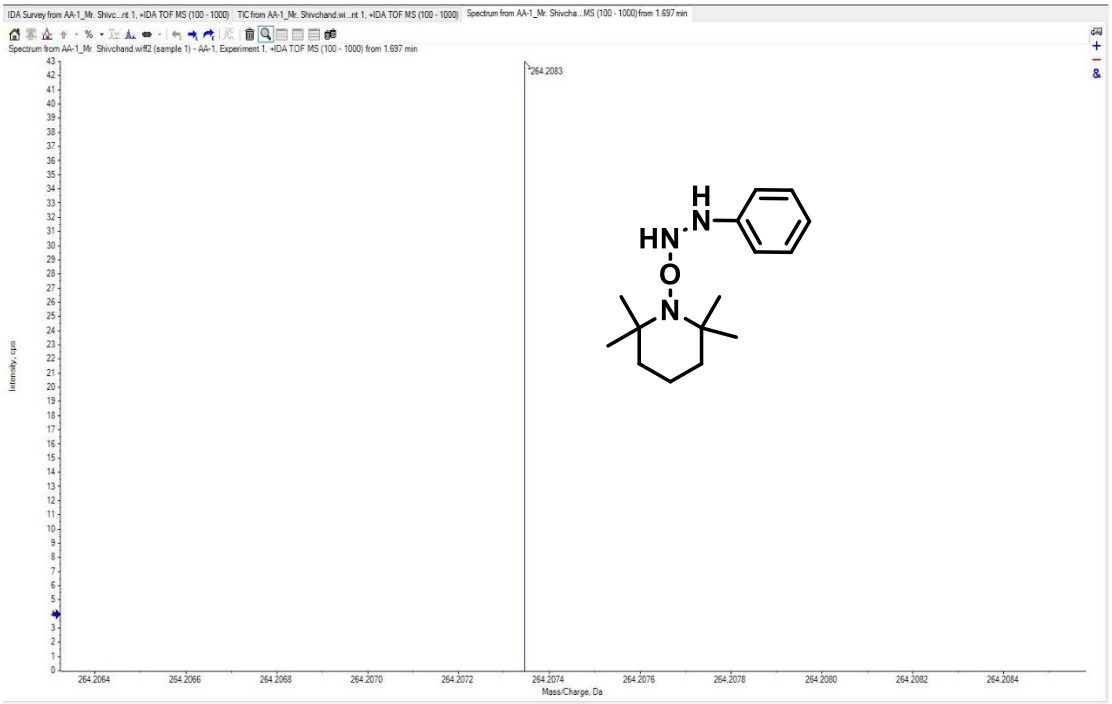

Figure 2.13 HRMS of adduct **7a**

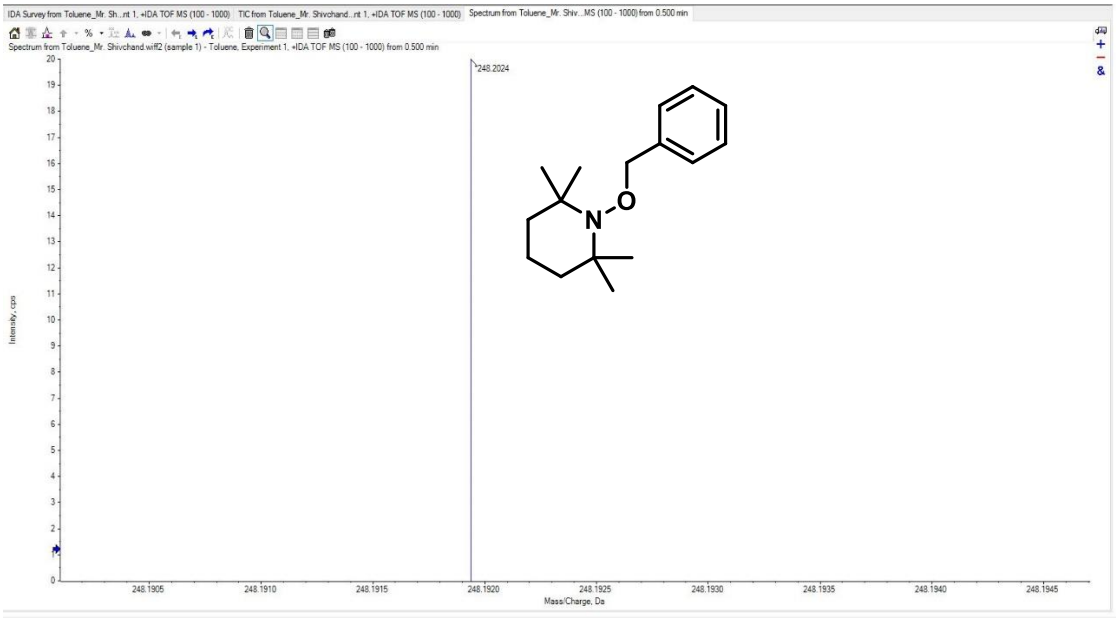

Figure 2.14 HRMS of adduct **8a**

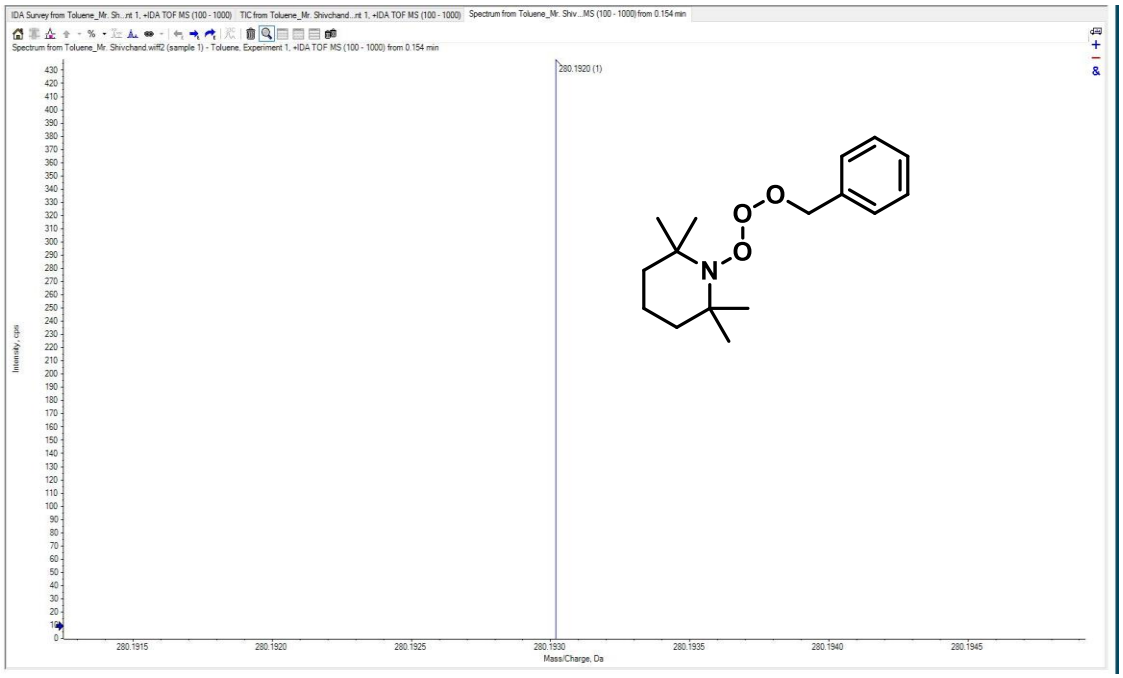

Figure 2.15 HRMS of adduct **9a**

2.10 References

[1] J.Y. Chen, W. Wu, Q. Li, W.T. Wei, Visible-Light Induced C(sp3)− H Functionalization for the Formation of C− N Bonds under Metal Catalyst-Free Conditions, Advanced Synthesis & Catalysis, 362 (2020) 2770-2777.
[2] D. Ma, Z. Zhang, M. Chen, Z. Lin, J. Sun, Organocatalytic Enantioselective Functionalization of Unactivated Indole C (sp3)− H Bonds, Angewandte Chemie, 131 (2019) 16063-16068.
[3] M.E. Hoque, M.M.M. Hassan, B. Chattopadhyay, Remarkably Efficient Iridium Catalysts for Directed C (sp2)–H and C (sp3)–H Borylation of Diverse Classes of Substrates, Journal of the American Chemical Society, 143 (2021) 5022-5037.
[4] J.-B. Chen, Y.-X. Jia, Recent progress in transition-metal-catalyzed enantioselective indole functionalizations, Organic & Biomolecular Chemistry, 15 (2017) 3550-3567.
[5] J.F. Hartwig, M.A. Larsen, Undirected, homogeneous C–H bond functionalization: challenges and opportunities, ACS central science, 2 (2016) 281-292.
[6] M. Kapoor, A. Singh, K. Sharma, M. Hua Hsu, Site-Selective C (sp3)− H and C (sp2)− H Functionalization of Amines Using a Directing-Group-Guided Strategy, Advanced Synthesis & Catalysis, 362 (2020) 4513-4542.
[7] A.A. Almasalma, E. Mejía, Recent Advances on Copper-Catalyzed C–C Bond Formation via C–H Functionalization, Synthesis, 52 (2020) 2613-2622.
[8] T. Gensch, M. Hopkinson, F. Glorius, J. Wencel-Delord, Mild metal-catalyzed C–H activation: examples and concepts, Chemical Society Reviews, 45 (2016) 2900-2936.
[9] C. Sambiagio, D. Schönbauer, R. Blieck, T. Dao-Huy, G. Pototschnig, P. Schaaf, T. Wiesinger, M.F. Zia, J. Wencel-Delord, T. Besset, A comprehensive overview of directing groups applied in metal-catalysed C–H functionalisation chemistry, Chemical Society Reviews, 47 (2018) 6603-6743.
[10] S.D. Tambe, R.S. Rohokale, U.A. Kshirsagar, Visible-Light-Mediated Eosin Y Photoredox-Catalyzed Vicinal Thioamination of Alkynes: Radical Cascade Annulation Strategy for 2-Substituted-3-sulfenylindoles, European Journal of Organic Chemistry, 2018 (2018) 2117-2121.
[11] B. König, Photocatalysis in organic synthesis–past, present, and future, European Journal of Organic Chemistry, 2017 (2017) 1979-1981.
[12] M.-j. Bu, G.-p. Lu, J. Jiang, C. Cai, Merging visible-light photoredox and micellar catalysis: arylation reactions with anilines nitrosated in situ, Catalysis Science & Technology, 8 (2018) 3728-3732.
[13] N.A. Romero, D.A. Nicewicz, Organic photoredox catalysis, Chemical reviews, 116 (2016) 10075-10166.
[14] S. Kumari, S. Kumar Maury, H. Kumar Singh, A. Kamal, D. Kumar, S. Singh, V. Srivastava, Visible Light Mediated, Photocatalyst-Free Condensation of Barbituric Acid with Carbonyl Compounds, ChemistrySelect, 6 (2021) 2980-2987.
[15] S.K. Maury, A.K. Kushwaha, A. Kamal, H.K. Singh, Visible light triggered synthesis of spiro [indoline-3, 4′-quinoline] via oxidative coupling of indole with enaminone and malononitrile, Journal of Molecular Structure, 1274 (2022) 134452.

[16] A. Kamal, H.K. Singh, S.K. Maury, S. Kumari, A.K. Kushwaha, V. Srivastava, S. Singh, Visible Light-Driven Synthesis of Amine–Sulfonate Salt Derivatives: A Step towards Green Approach, Journal of Molecular Structure, 1257 (2022) 132523.
[17] A. Kamal, H.K. Singh, D. Kumar, S.K. Maury, S. Kumari, V. Srivastava, S. Singh, Visible Light-Induced Cu-Catalyzed Synthesis of Schiff's Base of 2-Amino Benzonitrile Derivatives and Acetophenones, ChemistrySelect, 6 (2021) 52-58.
[18] X. Zhao, B. Li, W. Xia, Visible-light-promoted photocatalyst-free hydroacylation and diacylation of alkenes tuned by NiCl2· DME, Organic letters, 22 (2020) 1056-1061.
[19] V. Srivastava, P.K. Singh, S. Tivari, P.P. Singh, Visible light photocatalysis in the synthesis of pharmaceutically relevant heterocyclic scaffolds, Organic Chemistry Frontiers, 9 (2022) 1485-1507.
[20] H.K. Singh, A. Kamal, S. Kumari, D. Kumar, S.K. Maury, V. Srivastava, S. Singh, Eosin Y-catalyzed synthesis of 3-aminoimidazo [1, 2-a] pyridines via the HAT process under visible light through formation of the C–N bond, ACS omega, 5 (2020) 29854-29863.
[21] D.P. Hari, B. König, Synthetic applications of eosin Y in photoredox catalysis, Chemical Communications, 50 (2014) 6688-6699.
[22] Y. Jin, L. Ou, H. Yang, H. Fu, Visible-light-mediated aerobic oxidation of N-alkylpyridinium salts under organic photocatalysis, Journal of the American Chemical Society, 139 (2017) 14237-14243.
[23] M. Majek, F. Filace, A.J. von Wangelin, On the mechanism of photocatalytic reactions with eosin Y, Beilstein journal of organic chemistry, 10 (2014) 981-989.
[24] M. Rivas, V. Palchykov, X. Jia, V. Gevorgyan, Recent advances in visible light-induced C (sp3)–N bond formation, Nature Reviews Chemistry, 6 (2022) 544-561.
[25] L. Zheng, X. Zhuo, Y. Wang, X. Zou, Y. Zhong, W. Guo, Photocatalytic cross-dehydrogenative coupling reaction toward the synthesis of N, N-disubstituted hydrazides and their bromides, Organic Chemistry Frontiers, 9 (2022) 3012-3021.
[26] Y. Zhao, W. Xia, Recent advances in radical-based C–N bond formation via photo-/electrochemistry, Chemical Society Reviews, 47 (2018) 2591-2608.
[27] A.K. Bagdi, M. Rahman, D. Bhattacherjee, G.V. Zyryanov, S. Ghosh, O.N. Chupakhin, A. Hajra, Visible light promoted cross-dehydrogenative coupling: a decade update, Green Chemistry, 22 (2020) 6632-6681.
[28] N. Yadav, T. Khanam, A. Shukla, N. Rai, K. Hajela, R. Ramachandran, Tricyclic dihydrobenzoxazepine and tetracyclic indole derivatives can specifically target bacterial DNA ligases and can distinguish them from human DNA ligase I, Organic & biomolecular chemistry, 13 (2015) 5475-5487.
[29] L.A. Tatum, X. Su, I. Aprahamian, Simple hydrazone building blocks for complicated functional materials, Accounts of Chemical Research, 47 (2014) 2141-2149.
[30] M. Zhang, Z.-R. Shang, X.-T. Li, J.-N. Zhang, Y. Wang, K. Li, Y.-Y. Li, Z.-H. Zhang, Simple and efficient approach for synthesis of hydrazones from carbonyl compounds and hydrazides catalyzed by meglumine, Synthetic Communications, 47 (2017) 178-187.

[31] S. Devkota, S. Mohandoss, Y.R. Lee, Indium (iii)-catalyzed efficient synthesis of 3-arylhydrazonoindolin-2-ones and their fluorescent metal sensing studies, New Journal of Chemistry, 46 (2022) 3640-3644.
[32] S.K. Sridhar, M. Saravanan, A. Ramesh, Synthesis and antibacterial screening of hydrazones, Schiff and Mannich bases of isatin derivatives, European Journal of Medicinal Chemistry, 36 (2001) 615-625.
[33] S. Oezbey, A. Karayel, G. Kavak, Z. Seferoğlu, N. Ertan, X-Ray crystal structure analysis and determination of azo-enamine and hydrazone-imine tautomers of two hetarylazo indole dyes, Coloration Technology, 123 (2007) 358-364.
[34] Z.A. Kaplancıklı, L. Yurttaş, A. Özdemir, G. Turan-Zitouni, G.A. Çiftçi, Ş.U. Yıldırım, U.A. Mohsen, Synthesis and antiproliferative activity of new 1, 5-disubstituted tetrazoles bearing hydrazone moiety, Medicinal Chemistry Research, 23 (2014) 1067-1075.
[35] B. Evranos-Aksöz, S. Yabanoğlu-Çiftçi, G. Uçar, K. Yelekçi, R. Ertan, Synthesis of some novel hydrazone and 2-pyrazoline derivatives: Monoamine oxidase inhibitory activities and docking studies, Bioorganic & Medicinal Chemistry Letters, 24 (2014) 3278-3284.
[36] Y. Toledano-Magana, R. Melendrez-Luevano, M. Navarro-Olivarria, J.C. García-Ramos, M. Flores-Alamo, L. Ortiz-Frade, L. Ruiz-Azuara, B.M. Cabrera-Vivas, Synthesis, characterization and evaluation of the substituent effect on the amoebicide activity of new hydrazone derivatives, Medchemcomm, 5 (2014) 989-996.
[37] R. Kamal, V. Kumar, V. Bhardwaj, V. Kumar, K.R. Aneja, Synthesis, characterization and in vitro antimicrobial evaluation of some novel hydrazone derivatives bearing pyrimidinyl and pyrazolyl moieties as a promising heterocycles, Medicinal Chemistry Research, 24 (2015) 2551-2560.
[38] Y. Wang, X. Yu, X. Zhi, X. Xiao, C. Yang, H. Xu, Synthesis and insecticidal activity of novel hydrazone compounds derived from a naturally occurring lignan podophyllotoxin against Mythimna separata (Walker), Bioorganic & Medicinal Chemistry Letters, 24 (2014) 2621-2624.
[39] G. Rajitha, K.V. Prasad, A. Umamaheswari, D. Pradhan, K. Bharathi, Synthesis, biological evaluation, and molecular docking studies of N-(α-acetamido cinnamoyl) aryl hydrazone derivatives as antiinflammatory and analgesic agents, Medicinal Chemistry Research, 23 (2014) 5204-5214.
[40] M. Qin, T. Wang, B. Xu, Z. Ma, N. Jiang, H. Xie, P. Gong, Y. Zhao, Novel hydrazone moiety-bearing aminopyrimidines as selective inhibitors of epidermal growth factor receptor T790M mutant, European Journal of Medicinal Chemistry, 104 (2015) 115-126.
[41] T. Aysha, A. Lyčka, S. Luňák Jr, O. Machalický, M. Elsedik, R. Hrdina, Synthesis and spectral properties of new hydrazone dyes and their Co (III) azo complexes, Dyes and Pigments, 98 (2013) 547-556.
[42] S.E. Denmark, W.-T.T. Chang, K. Houk, P. Liu, Development of chiral bis-hydrazone ligands for the enantioselective cross-coupling reactions of aryldimethylsilanolates, The Journal of organic chemistry, 80 (2015) 313-366.

[43] C.-r. Li, Z.-c. Liao, J.-c. Qin, B.-d. Wang, Z.-y. Yang, Study on 2-acetylpyrazine (pyridine-2′-acetyl) hydrazone as a fluorescent sensor for Al3+, Journal of Luminescence, 168 (2015) 330-333.
[44] A. Gusev, A. Mazinov, A. Tyutyunik, I.S. Fitaev, V. Gurchenko, E. Braga, Effect of Doping with N, Br, and F Atoms on Electrodynamic Characteristics and Physical Properties of Isatin-β-anil, Technical Physics, 66 (2021) 84-92.
[45] M. Cigáň, K. Jakusová, M. Gáplovský, J. Filo, J. Donovalová, A. Gáplovský, Isatin phenylhydrazones: anion enhanced photochromic behaviour, Photochemical & Photobiological Sciences, 14 (2015) 2064-2073.
[46] Y. Ding, H. Li, Y. Meng, T. Zhang, J. Li, Q.-Y. Chen, C. Zhu, Direct synthesis of hydrazones by visible light mediated aerobic oxidative cleavage of the C [double bond, length as m-dash] C bond, Organic Chemistry Frontiers, 4 (2017) 1611-1614.
[47] Y. Kong, K. Wei, G. Yan, Radical coupling reactions of hydrazines via photochemical and electrochemical strategies, Organic Chemistry Frontiers, 9 (2022) 6114-6128.
[48] A.K. Kushwaha, S.K. Maury, S. Kumari, A. Kamal, H.K. Singh, D. Kumar, S. Singh, Visible-Light-Initiated Oxidative Coupling of Indole and Active Methylene Compounds Using Eosin Y as a Photocatalyst, Synthesis, 54 (2022) 5099-5109.
[49] M. Uygur, J.H. Kuhlmann, M.C. Pérez-Aguilar, D.G. Piekarski, O.G. Mancheño, Metal-and additive-free C–H oxygenation of alkylarenes by visible-light photoredox catalysis, Green Chemistry, 23 (2021) 3392-3399.
[50] R. Li, T. Shi, X.-L. Chen, Q.-Y. Lv, Y.-L. Zhang, Y.-Y. Peng, L.-B. Qu, B. Yu, Visible-light-promoted organic dye-catalyzed sulfidation and phosphorylation of arylhydrazines toward aromatic sulfides and diarylphosphoryl hydrazides, New Journal of Chemistry, 43 (2019) 13642-13646.